Lawrence Berkeley National Laboratory

Title
EFFECT OF GRAIN SIZE ON THE MECHANICAL PROPERTIES OF DUAL PHASE Fe/Si/C STEELS

Permalink
https://escholarship.org/uc/item/2fj9603p

Author
Ahn, J.-H.

Publication Date
1983-08-01

Lawrence Berkeley Laboratory

UNIVERSITY OF CALIFORNIA

Materials & Molecular Research Division

EFFECT OF GRAIN SIZE ON THE MECHANICAL PROPERTIES
OF DUAL PHASE Fe/Si/C STEELS

J.-H. Ahn
(M.S. Thesis)

August 1983

DISCLAIMER

EFFECT OF GRAIN SIZE ON THE MECHANICAL PROPERTIES
OF DUAL PHASE Fe/Si/C STEELS

\)

Jae-Hwan Ahn

M.S. Thesis

August 1983

Lawrence Berkeley Laboratory
University of California
Berkeley, California 94720

EFFECT OF GRAIN SIZE ON THE MECHANICAL PROPERTIES

OF DUAL PHASE Fe/Si/C STEELS

Table of Contents

EFFECT OF GRAIN SIZE ON THE MECHANICAL PROPERTIES

OF DUAL PHASE Fe/Si/C STEELS

Jae-Hwan Ahn

Materials and Molecular Research Division
Lawrence Berkeley Laboratory
and Department of Materials Science and Mineral Engineering
University of California,Berkeley,California 94720

ABSTRACT

The present investigation is concerned with the influence of the prior austenite grain size on the mechanical properties of dual phase ferrite-martensite (DFM) steels. The steel used in this investigation is an Fe/2Si/0.1C alloy with an intermediate quenching heat treatment. It was found that as the prior austenite grain size is refined, significant improvements in total elongation, reduction in area and impact toughness can be acheived, while uniform elongation, yield and tensile strengths are not affected. These improvements are analyzed in terms of microstructure and fracture characteristics.

Careful observations of the microcracks and fracture profile shows the cleavage cracks propagate nearly straight without deviation at the ferrite/martensite interfaces within the sub units of the DFM structure, but change their path at high angle sub-unit boundaries. The crack is less likely to be deflected at the ferrite/martensite interface because the interface is coherent. In this investigation, the sub-unit of the DFM structure is defined as the area of aligned fibers of martensite and ferrite, having nearly the same crystallographic orientation throughout. This sub-unit is directly related to the prior

martensite packets, and thus is controlled by the prior austenite grain size.

A comparision of optical micrographs and SEM fractographs has shown that there is close agreement between the sub-unit size and cleavage facet size. All of the observations above lead to the quantitative conclusion that the sub-unit size is the basic microstructure unit controlling the fracture behavior of DFM steels produced by the intermediate quenching heat treatment. Consequently, it is expected that the fracture energy will be improved by refining the sub-unit size of DFM steels, i.e., the prior austenite grain size.

Thus, a controlled rolling process was undertaken to obtain grain refined DFM steels. The results showed that this process is an effective way to obtain micro-duplex structures with attractive mechanical properties in an economical way. The considerable improvements in mechanical properties obtained are attributed to the ferrite grain refinement through the hot rolling process. Different processing conditions lead to variations in the relative amounts of micro-constituents, which corelate well with variations in strength, ductility and impact toughness.

PART ONE – INTERMEDIATE QUENCHING TREATMENT

I. Introduction

The need for economical, higher strength steels with good formability in transportation industries to achieve weight reductions and fuel savings has spurred intensive development programs in the area of low-carbon, low alloy steels. Many design goals have been met by conventional high strength, low-alloy (HSLA) steels which derive principal strengthening from finely dispersed alloy carbides and through grain refinement. However, their overall mechanical properties are not satisfactory for applications, such as extensive cold forming, especially when alloying and processing economics are considered [1]. Hence, recent emphasis has been placed on low carbon dual-phase (duplex ferritic-martensitic) steels as a viable alternative due to their attractive combinations of strength and formability [2-4]. These optimum mechanical properties are achieved in essence by the production of microstructures containing inherently strong load carrying martensite in a relatively soft ferrite matrix.

The ongoing duplex ferritic-martensitic (DFM) steel design program at UC Berkeley, has produced a fundamental understanding of the origin and the characteristic mechanical behavior of several DFM steel alloys and has shown the effects of different metallurgical variables such as the volume fraction [5], morphology [6], and carbon-content [7], of the martensite and alloying elements [8,9]. The characteristic behavior of dual

phase steels are high work hardening rate, continuous yielding, high tensile/yield strength and good elongation to necking. These characteristics are indicative of excellent formabiltiy in combination with high strength. The origin of these characteristics has been attributed to the presence of mobile dislocations in the ferrite matrix near the ferrite/martensite interface. These dislocations are by-products of the austenite to martensite transformation during quenching after two-phase annealing.

Though a great deal of work has been carried out to understand the origin and the characteristic mechanical behavior of DFM steels, the effect of grain size on the mechanical properties is not well established. It has been well recognized that grain size is one of the most important metallurgical parameters in controlling the strength and associated ductility of low-carbon steels [10-12]. Grain size refinement has been exercized in numerous systems particularly because of the benefit of improving ductility and toughness without a sacrifice in strength. Also, in steels hardened by heat treatment, a strengthening effect through the refinement of the prior austenite grain size has been demonstrated [13]. The basic microstructural unit controlling the strength and fracture of lath martensite, analogous to grain size in ferrite, has been reported to be packets [14-16], or blocks [17], the size of which is controlled by the prior austenite grain size.

As part of an ongoing research program on the relation between microstructure and mechanical properties in DFM steels,

the purpose of the present investigation is to determine the effect of refinement of prior austenite grains on the mechanical properties of dual-phase Fe/Si/C steels obtained by the intermediate quenching process (5), and to obtain the fundamental information necessary to improve the strength and toughness through microstructural manipulation.

II.   Experimental Procedure

A.   Materials Preparation

The alloy used in this investigation was a high purity Fe/1.9%Si/0.13%C steel. The 20 pound cylindrical ingots were melted in a vacuum induction furnace at Lawrence Berkeley Laboratory. They were subsequently homogenized at 1200°C under argon atmosphere for 20 hours, followed by upset forging and cross rolling into bars of 5/8 in. x 2-3/4 in. cross section. All of the above treatments were followed by air cooling. Oversized round tensile and Charpy impact specimen blanks were cut with their axes parallel to the longtudinal direction of the bars.

B.   Heat Treatment

For the purposes of this investigation, the intermediate quenching heat treatment was chosed from among the many heat treatments available for producing a DFM microstructure. It was chosen because it has been shown previously to produce a microstructure with favorable mechanical properties (6). Oversized round tensile and Charpy impact specimen blanks were austenitized in a vertical tube furnace under flowing argon atmosphere for one hour at 1100°C and quenched directly into agitated iced water. After obtaining a fully martensitic structure, the specimens were annealed in the (α+γ) region for ten minutes and once again quenched into agitated iced water.

The two-phase annealing temperatures were chosen so as to obtain the required volume fraction of martensite as shown in Table I. To investigate the effect of the prior austenite grain size on the mechanical properties of 2% Si DFM steels, the modified heat treatment has a second austenitizing and quenching treatment before two-phase annealing. This results in significant refinement of the prior austenite grains.

Based on optical metallography, the second austenitizing treatment was performed at $20^{\circ}C$ above A_3 temperature ($\gamma-$ solidus) for 8 minutes, which is a suitable holding time. The A_3 temperature was determined to be $980^{\circ}C$ after extensive heat treatment experiments near A_f temperature. The schematic diagram in Fig. 1 portrays the conventional duplex thermal treatment used in this study as well as the modified grain refining treatment, along with the Fe-rich portion of the 2% Si section of the Fe/Si/C phase diagram.

C.   Mechanical Testing

1.   Tensile Test

Tensile properties were determined using one-inch gauge length round tensile specimens as shown in Fig. 2. Oversized specimen blanks were heat treated and ground to final dimension following ASTM specification [18]. Approximately 0.05 inches of material was removed circumferentially around the gauge section to eliminate the possible effects of surface decarburization.

Tensile tests were performed at room temperature on an Instron testing machine with a cross-head speed of 0.02 inch/minute and a full scale load of 10,000 lbs. Total elongation was determined by measuring 1" marks on the gauge before and after testing with an optical microscope equipped with a Vernier translating stage accurate to 0.001 in. The reduction in area calculations is based on measurements of the gauge section diameter before and after testing. The rest of the properties were determined from the curves produced by the testing machine's chart recorder. The values of the tensile properties reported in Table l are the averages of the three test.

2. Charpy Impact Test

Impact properties were determined using the standard Charpy V-notch specimens shown in Fig. 2. Three or four specimens were tested for each heat treatment and data points were taken as the averages of these. Impact tests were performed using a Universal impact machine with calibrated unites of 0.25 ft-lbs. Low and high temperature tests were conducted according to ASTM specifications (19). To obtain zero and sub zero temperatures, various proportions of ethyl alcohol and dry ice were used. Charpy specimens were immersed in these mixtures and kept there for a sufficiently long time to obtain the required temperature before testing. For above room temperature tests, a

thermostatically controlled oil bath was used.

D.   Metallography

1. Optical Metallography

Samples for optical metallography were cut from 100% martensitic bulk specimens and from the fractured tensile and impact specimens under flood cooling. After mounting in either Bakelite or Koldmount, the specimens were mechanically ground successivley on wet emery paper from 180 to 600 grit. Final polishing was done with 1 μm diamond polish with kerosene as a lubricant. In these metallographic investigations the standard etchants, 2% and 5% Nital, were used to reveal the duplex microstructural features. Prior austenite grain boundaries were revealed by immersion in an etching solution of 1g picric acid, 1g dodecylbenzene sulfonate and 100 mL of water. Samples were examined on a Zeiss Ultraphot II metallograph.

2. Transmission Electron Microscopy

Thin foils for TEM were obtained from the tensile and impact specimens. Slices of about 20 mils thick were cut longitudinally from these specimens under flood cooling to minimze specimen heating. These slices were then chemically thinned to about 5 mils thick in a solution of H_2O_2 containing 2% HF at room temperature. 3.0 mm-dia. discs were spark cut from these thinned

slices and then mechanically ground to a thickness of about 2 mils and cleaned with acetone. Final thinning was done in a twin-jet electropolishing apparatus at room temperature using a chromic-acetic acid soltuion consisting of 75 gm CrO_3, 400 mL CH_3COOH and 21 mL distilled water. Polishing times varied from 3 to 5 min. at 50~55 ma and 40~45 volts. Foils were examined in a a JEM-7A electron microscope at an acceleration voltage of 100KV.

3. Scanning Electron Microsopy

The fracture morphology was thoroughly examined on the fracture surfaces of broken tensile and Charpy specimens using an ISI DS-130 scanning electron microscope operated at 25KV. Fracture surfaces selected for examination were cut, ultrasonically cleaned and stored in a dessicator until examination. A number of the fracture surfaces were nickel plated for examination in cross-section. Examination was done on the polished and etched section of the fracture profile to investigate the influence of microstructure of DFM steels on the fracture behavior.

III. Results and Discussion

A.   Microstructure

1. Initial Martensite

The production of a microstructure consisting of martensite dispersed in a ferrite matrix can be produced via many different heat treatments, all of which involve phase transformation in the $(\alpha+\gamma)$ region. The choice of the specific heat treatment will depend on the alloy composition, property requirements and production capabilities. In this investigation the intermediate quenching heat treatment was adopted so as to fully exploit the characteristic nature of the initial martensite structure prior to subsequent annealing in the $(\alpha+\gamma)$ range. This structure has been shown to be favorable for austentite nucleation on a fine scale during two-phase annealing because of the numerous fine heterogeneities in the structure [20]. It has been also recognized that martensite is a desirable microstructure for grain refinement by simple austenitizing thermal cycling [21].

The initial as-quenched martensitic structures and prior austenite grain sizes of the DFM steel before two phase annealing are shown in Figs. 3 and 4. The microstructure was completely martenistic without any evidence of proeutectoid ferrite which may have been produced during quenching (Fig. 3). In Fig. 4., it is also evident that the prior austenite grain size (heat treatment A) is refined by the second austenitizing cycle (heat

treatment B). For both treatments, the prior austenite grain is partitioned into several packets which consist of parallel highly dislocated laths, typical of low-carbon martensite. Each lath forms directly from an independent homogeneous shear and successive shear transformation produce a packet [22]. The lath boundaries are believed to be frequently of low angle characater, whereas the packet boundaries are usually high angle [23,24]. The effect of prior austenite grain size on the packet size is shown in Table III. As the austenite grain is varied from 200 μm to 60 μm , the packet size is changed from 80 μm to 30 μm. This result is similar to that obtained for martensite in Fe-0.2C alloy by T. Maki et al.[25]. The average size of austenite and packet are established by linear intercept measurements on optical microscopy [26].

Careful transmission electron microscopy studies of the initial martensite for both heat treated specimens showed there is no observable variation in the morphology and the substructure of the martensite because of the difference in the prior austenite grain size. Figure 6 shows a typical initial microstructure before two-phase annealing, which consists almost entirely of dislocated laths on the order of 0.1 μm to 1.0 μm in width. The existence of retained austenite was expected since its presence in such low carbon steels had been detected earlier [5,27]. The narrow films of retained austenite trapped between the growing martensite laths in the form of narrow thin films were identified by indexing selected area diffraction patterns. Fig. 7 shows the crystallographic relation between austenite and

martensite, which exhibits the Kurdjumov-Sachs orientation relationship $\langle 111 \rangle_\alpha / \langle 110 \rangle_\gamma$.

From these optical and transmission electron micrographs, the initial marteniste structures before being subjected to two-phase annealing are similar except for the packet size, indicating that the lath martensite structure itself is not affected by the austenite grain size at least in the range of the present investigation.

2. Duplex Microstructure

During annealing of the initial marteniste in the $(\alpha+\gamma)$ region, the martensite transforms partially to austenite and the residual regions become ferrite as the two phases attain the volume fractions specified by the tie line corresponding to the holding temperature. The alloy phases will then consist of low carbon ferrite and higher carbon austenite. Upon final quenching, the austenite transforms to martensite and the ferrite regions become heavily dislocated as a result of accommodating the martensite transformation strain. Fig. 5 shows the DFM structure, the needle-like particles of light contrast correspond to martensite in the grey ferrite matrix.

As observed earlier [5], there was no evidence of the nucleation and growth of austenite particles along the prior austenite grain boundaries. Evidently these needle-like particles nucleate and grow along initial martensite lath boundaries. This is relaxation of classical nucleation theory [28], which states that the preferred sites for austenite

formation are prior austenite grain boundaries, martensite lath boundaries, and possibly other lattice defects.

As a plausible explanation for this phenomenon, Koo has postulated the occurrence of Si segregation along the prior austenite grain boundaries during solution treatment [5]. Therefore, austenite nucleation at the prior austenite grain boundaries will be prevented by the repellent interactions between carbon and the preoccupied silicon atoms at the boundaries [29], and will occur at the initial marteniste lath boundaries. For the Si effect on the austenite growth he has also postulated that the Si concentration "spike" at the interface between austenite and ferrite will act as a barrier to carbon diffusion because of the repellent interaction between carbon and silicon. As a result, lateral thickening of the austenite particles will be restricted at the martensite lath boundaries where the diffusion of carbon is more rapid along the lath boundaries where the diffusion of carbon is more rapid by the lath boundary diffusion and hence austenite growth can occur. Consequently, a completely needle-like morphology along martensite lath boundaries was adopted for the formation of austenite from the martensite structure during two-phase annealing. Quenching to room temperature transforms the austenite to martensite, resulting in the fine fibrous martensite in the ferrite matrix.

From Fig. 5, it can be noticed that the influence of austenite grain size and packet size is clearly reflected in the fine, acicular DFM structure. The DFM structural sub-unit, which

is the area of aligned fibers of martensite and ferrite, is refined without changing the interparticle (martensite) spacings at the same volume fraction of martensite. This result was expected, since upon two phase annealing the austenite nucleates and grows along prior lath martenstie boundaries and forms the parallel accicular austenite pools within the prior packet. Careful observation by optical microscopy of the initial martensite and DFM structure shows that the average size of the sub-unit in DFM structure which is shown in Table III corresponds almost exactly to the packet size of initial martensite before two phase annealing, and is a function of prior austenite grain size. Apart from the sub-unit size in the DFM structure, the geometrical features of the DFM structure remain largely unchanged as the prior austenite grain size is varied.

The morphology of the martensite in these DFM structures also consists of dislocated lath martensite and did not differ significantly from the fully martensite, except some area of twinning in substructure due to the increase of carbon amount. The morphology of the ferrite region is similiar in all the DFM structures and is associated with fine subgrain and high dislocation density near the ferrite/martensite interface, as shown in Fig. 8.

B.   Mechanical Properties

1.   Tensile Properties

The room temperature tensile test data of the as-quenched DFM steels are summarized in Table I. At the same prior austenite grain size, the effect of the volume fraction of martensite on the values of strength and ductility obey the two phase mixture rule as demonstrated in many dual phase systems [5,30]. Figs. 9 and 10 show the effect of prior austenite grain size on the strength and elongation of DFM steels at each volume fraction of martensite. While the variation of prior austenite grain had little effect on the tensile strengths and uniform elongation, considerable changes occurred in total elongtion with austenite grain refinement. Reduction in area was increased significantly with austenite grain refinement. However, the values of the reduction in area remain relatively unchanged over different volume fractions of martensite at the same prior austenite grain size.

2. Impact Properties

Charpy V-notch impact tests were conducted to determine the influence of volume pct. martensite and prior austenite grain size on the ductile to brittle transition temperature (DBTT). The results of the impact tests are summarized in Table II. The data reported represent an asverage of at least three tests. Figs. 11 and 12 show the impact energy curves of the as-quenched DFM steels with the prior austenite grain size. These curves do not exhibit a sharp DBTT. However, it is evident that fine-grained specimens have lower DBTT than course-grained specimens for all volume fractions of martensite tested. From Table III

one can also observe that there is no significant difference in the impact energy as the volume fraction of martensite varied at the same austenite grain size.

C.   Fractography

The fracture mode of the broken tensile specimens for coarse and fine grain are predominantly dimple rupture, indicating stable, subcritical crack extension (Fig. 13). The fracture surfaces of broken Charpy impact specimens tested at 0^oC are shown in Figs. 14 and 15 and demonstrate the effects of prior austenite grain size of DFM steels on the fracture surface. For both fine grained and coarse grained DFM steels, the mode of fracture is mostly associated with a large proportion of quasi-cleavage produced by a high deformation rate due to impact loading. In all cases, the small cleavage facets are separated by tear ridges and contain river pattern and cleavage tongues. It is clearly seen that fracture surface of the large austenite grained specimen (Figs. 14-a and 15-a) consist of large and rather flat fracture facets as a whole, although many small cleavage steps or tear ridges are observed. In contrast, the facets for the small austenite grained specimen are small. As the testing temperature is raised to 50^oC, there is a change in fracture mode from brittle cleavage to ductile dimple for specimens having a fine austenite grain size. (Fig. 16-b). However, Fig. 16-a shows there is no change in fracture mode for coarse grained specimens at this temperature.

It has been generally accepted that the fracture plane

changes its orientation at high angle grain boundaries, resulting in quasi-cleavage facets whose average size is essentially identical with that of a division of microstructure by the groups of the same orientation [31,32]. From this consideration it is interesting to correlate the fracture facet size with the microstructure of DFM steels. By comparing the optical microscopy and fractography, the average facet size is found to be almost identical to the size of the 'sub-unit' of DFM steels mentioned earlier and the packet size of the initial martensite. Therefore, it is seen that the average cleavage facet size (which seems to be related to the fracture behavior of DFM steels) is a function of the prior austenite grain size. The average sizes of the cleavage facets were measured by the spacings between two neighboring heavy tear lines of the fracture surface by linear analysis [26], and are listed in Table III.

Figure 17 shows where the void/micro crack forms first in DFM steels. This micrograph was taken at the necked region of a broken tensile specimen. A large density of void nucleation was found near the martensite-ferrite interface, but not in the martensite. At present this phenomenon may be explained in part due to the difference in the flow strengths of ferrite and martensite. The distribution of stress and strain is very inhomogeneous during deformation of DFM steels, resulting in localized deformation and/or stress concentration in the area of ferrite near martensite. Consequently this leads to the fracture of the ferrite. The propagation of the crack through DFM steels is shown in Fig. 18, which is taken from the fractured impact

specimen tested at -50°C. It is clearly seen that the cleavage crack runs nearly straight in the sub-unit of DFM steels and is arrested by neighboring sub-unit. No apparent change in the fracture appearance was noticed with regard to the volume fraction of martensite in this investigation.

D.   Microstructure/Mechanical Property Correlation

By examining the corresponding mechanical properties obtained from both heat treatments, the specimen subjected to grain refinement displayed improvements in total elongation, impact toughness and reduction in area, while uniform elongation, yield and tensile strengths are not affected. These differences in mechanical properties must be related to the effect of prior austenite grain size since all other metallurgical variables in the two specimens are virtually identical. It is well known that total elongation includes both the uniform elongation, which is dependent on work hardening rate, and the fracture strain which relates to the crack path progress [33]. Thus the only difference ductility for both fine and coarse grained specimen is the fracture strain. From this consideration the improvement of fracture strain and impact toughness with austenite grain refinement could be analysed in terms of fracture characteristics.

It is well known that one of the most important factors controlling the toughness of a ferritic steel is the grain size, in which the crack front propagates nearly straight within a

grain and changes its direction at the grain boundary because of the change in crystallographic orientation [31]. Since the fracture mode of DFM steels is similar to that of ferritic steel, it is expected that the natural choice of micro structural unit contolling the fracture may be a region bounded by high angle boundaries in which cleavage cracks propagate without deviation.

With the experimental results and micrographs described earlier, it is possible to define such a region in DFM steels used in this investigation. By comparing the optical microscopy and fractography, as listed in Table III, it was found there is close agreement between the packet size of initial martensite, the sub-unit size of DFM structure and the cleavage facet on the fractured impact specimen. This close agreement between them strongly implies the dominant microstructural unit relevant to the cleavage fracture of DFM steels is the size of the sub-unit, i.e., the initial martensite packet. Further evidence to verify the improvement in fracture strain and impact toughness with prior austenite grain refinement can be provided by examination of the cross section of nickel plated fracture surfaces of DFM impact specimen tested at $-50^{\circ}C$. With this technique the relationship between the microstructure and fracture behavior of DFM steels can be correlated. An example of micro cracks found below the main crack front is shown in Fig. 18. A cleavage crack runs nearly straight in the sub-unit of DFM steels without deviation and is stopped by the sub-unit boundary which corresponds to be the high angle packet boundary in the initial martensite structure. It appears that the propagation of a

cleavage crack across the sub-unit boundary requires the initiation of a new crack in the neighboring sub-unit. This phenomenon is similar to that of a high-angle grain boundary in ferritic steel. The reason why the crack of the DFM alloys propagates nearly straight without deviation at the ferritic/martensitic interface within a sub-unit can be explained as follows. At present, the most plausible explanation of this phenomenon could be in part due to the good atomic fit across the ferrite/martensite interface. During two phase annealing the austenite nucleates and grows along prior lath boundaries and forms the accicular austenites within the packet. Upon quenching, the austenite tends to transform to the same variant as the previous martensite. Since the ferrite regions are essentially tempered martensite, the entire sub- unit is of nearly the same crystallographic orientation and ferrite-martensite boundaries are also of very low angle.

Fig. 20 (courtesy of J.Y. Koo [5]) shows the conventional bright field (a) and corresponding high resolution lattice fringe image (b) of a ferrite/martensite interface in the 2%Si/0.06%C DFM steel. As the (110) fringes cross the interface, they are distorted but are continuous except for occasional end-on dislocation. Thus the advancing crack is less likely to be deflected from its path at the interface, resulting in very little energy consumption during crack propagation across the ferrite/martensite interface. This, in turn, can result in easy crack propagation in the sub-unit area of DFM steels.

An example of the fracture surface profile is shown in Fig.

19, which shows that the cleavage cracks are nearly straight through the sub-unit regions but change their direction at high-angle sub-unit boundaries. Careful examination of the short straight segments composing the main fracture profile shows that the length of this segment, i.e., unit crack, corresponds almost to the average sub-unit size of DFM structure.

Considering the aspects of crack propagation in DFM steels, the 'sub-unit' size of DFM structure appears to play an important role in controlling fracture energy, since the sub-unit size is directly related to the cleavage facet size. Consequently, it may be reasonable to be considered that structural unit controlling fracture (especially the cleavage fracture) is the martensite packet, which, in turn, is controlled by the prior austenite grain size. These fracture characteristics are analogous to the results in the tempered martensite of low carbon nickel steel by T. Inoue et al. [17] and Fe-Mn martensite by M. J.Roberts [14]. They may have shown that the dominant factor leading to the ultimate cleavage fracture is the mean length of the packet, which is varied considerably with the prior austenite grain size. All of the above observations lead to the qualitative conclusion that by refining the prior austenite grain size before two-phase annealing, the improved total elongation and impact toughness are expected at least in the range of present investigation and for the intermediate quenching treatment.

PART TWO – THERMOMECHANICAL TREATMENT

I. Introduction

The previous chapter has shown that the fracture behavior of DFM steel is controlled by a basic microstructural unit having the same crystallographic orientation throughout, and suggested the beneficial effect of fine grain size for the desirable mechanical properties. It has been amply demonstrated that strain hardening of austenite by deformation, e.g. by controlled rolling that takes place either prior to or during the austenite-ferrite transformation leads to a significant decrease in grain size [34]. In order to realize the full potential of this process, information is being obtained about a number of properties of engineering significance. The controlled rolling process consists of heating the steel to an optimum soaking temperature, deforming above and below the austenite recrystallization temperature, and/or deforming in the austenite-ferrite two phase range. Fine ferrite grain size can be produced on transformation from austenite which remains unrecrystallized after hot-rolling and optimum grain size can be obtained by careful control of processing variables, especially deformation and temperature conditions.

As a step toward providing a fine grain DFM structure, the present work was undertaken to demonstrate how thermomechanical procssing might be used to obtain as-hot-rolled DFM structure and to improve the mechanical properties in the low carbon silicon steel. Moreover, hot rolling could be an economical process of

heat treatment, as a continuous process saves energy otherwise needed to reheat the material.

II.   Experimental Procedure

The alloy used in this investigation was a high purity Fe/2.1%Si/0.11%C steel, which was supplied by Nippon Kokan K. K. in the form of 1" dia. hot-rolled bars. For thermomechanical process a test material was soaked at 1150°C for 30 minutes, then rolled down to 0.625" dia. bar in two passes on a two-high reversing bar mill. After deformation, the bar was annealed in the $(\alpha+\gamma)$ region for 10 minutes and finished rolled to 0.5" dia. bar followed by water quenching or air cooling. The finishing rolling temperature was chosen similar to those commonly used on conventional hot working practice. Tensile and Charpy specimens were machined from these heat treated bars in the longitudinal direction.

Another heat treatment, step annealing, was conducted to determine the deformation effect on mechanical properties of DFM steel. This was done by austenitizing the machined tensile and Charpy specimens at 1150°C for 30 minutes and then tranferring directly to an adjacent furnace at the desired two phase temperature and holding for 10 minutes. Then specimens were directly water quenched or air cooled. The schematic diagrams of heat treatment used in this part of the research are illustrated in Fig. 21.

III.   Results and Discussion

A.   Microstructure

In this section, the initial phase before two phase annealing is austenite. Upon decreasing the temperature to the two phase range, ferrite nucleates at the prior austenite grain boundaries and grows into the austenite [35,36]. The microstructure thus depends on the prior austenite grain size.

The optical microstructure by step annealing process is shown in Fig. 22a (air cooled) and Fig. 22b (water quenched). The microstructural features are coarse two phase aggregates of large irregular shaped second phase in the coarse ferrite matrix, which shows the influence of the large austenite grain before two phase annealing.

Fig. 23 shows the optical microstructure for the hot rolled and air cooled specimens and Fig. 24, for the hot rolled and water quenched conditions. From these micrographs it can be seen that thermomechanical treatment has a strong influence on the grain size. For the thermomechanically treated steels, the coarse austenite obtained by soaking at 1150°C is broken into small recrystallized austenite through hot rolling in the austenite region, resulting in fine duplex structure after two phase annealing. When the alloy is further deformed after two phase and directly quenched/air cooled, the dual phase structure is developed in which the second phase is more or less unidirectionally aligned in the ferrite matrix. TEM studies

revealed that the nature of the second phases was mainly lath martensite substructure for water quenching and pearlite for air cooling, which is shown in Fig. 25, regardless of hot rolling or step annealing. The ferrite areas for the hot-rolled and water quenched material showed a high density of dislocations and less recovery due to the deformation in the $(\alpha+\gamma)$ region followed by fast cooling (Fig. 26-a) while in the hot rolled and air cooled condition, ferrite grains consisted of areas of coarse ferrite and areas of recovered or recrystallized ferrite as shown in Fig. 26-b.

B.   Mechanical Properties

The mechanical properties of tensile and Charpy test are summarized in Tables IV and V, and are presented graphically in Figs. 27 and 28. Comparing the values of mechanical properties between hot-rolled and step annealed materials, one observes that the former provided better combinations of mechanical properties than the latter treatments. The improvement in mechanical properties through the thermomechanical treatment can be correlated with the fine grain size which is the main microstructural change.

The effect of the ferrite grain size on the flow stress of a material is generally described by the Hall-Petch equation [37,38], $\sigma_f = \sigma_0 + kd^{-1/2}$ where σ_f is the flow stress at constant strain, d is the grain size and σ_0, k are material constants. Since the ferrite region obtained by thermomechanical treatment

was fine, the ferrite would be effectively strengthened according to the Hall-Petch equation. This effect appears to be mainly responsible for higher strength obtained by hot rolling process compared to step annealing for all air cooled specimens. From Table IV, one can notice that the strength of air cooled specimen is increased with decreasing the temperature of finish rolling, presumable because of the finer ferrite grain size (Fig. 23). This result is similar to those observed by T. Tanaka et al.[39].

For water quenching treatment, there was less difference in tensile strength between specimens given hot rolling and step annealing. This could be understood from the fact that the specimen given step annealing and water quenching has higher volume fraction of martensite and large martensite size. In DFM steels it has been shown that tensile strength is increased with the volume fraction of martensite and large size of martensite develops higher strength at the same volume fraction of martensite [6]. Thus the increase in the strength by ferrite grain refinement balances the increase in strength by high volume fraction of martensite and coarser martensite size. For the hot rolled and water quenched material the decrease in strength after lower finishing rolling temperature is due to the decrease in volume fraction of martensite as observed in many dual phase steels [5,30](Fig. 24).

There was considerable increase in ductility and impact toughness through hot-rolling, which could be analyzed in terms of ferrite grain size and fracture characteristics. The fracture surface of the broken tensile specimen for water quenching is

shown in Fig. 29. Coarse dual phase structures fracture predominantly by cleavage as revealed by well-defined facet, while fine structures fracture in ductile manner. The fracture mode of broken Charpy impact specimens tested at room temperature for water quenching is shown in Fig. 30 and demonstrates the effect of grain size. It is clearly seen that fracture surface of step annealed are composed of large and undistorted cleavage facet, which reflect a low resistance to fracture. In contrast the cleavage facet of the specimen which had been subjected to hot rolling is very small. As pointed out in the previous chapter, the crack front propagates nearly straight within the area of the same crystallographic orientation (effective grain), and will be stopped by the effective barrier. As a result the crack is forced to reinitiate repeatedly, and considerable energy is expended as it alters direction in search of the most likely propagation plane in the continuous grain. Therefore, the crack front of fine grain structure changes its direction more often, resulting in a significant improvement of the toughness of the material. Further evidence of the resistance to crack propagation of ferrite grain boundaries is given in Figs. 32 and 33, in which microcrack and fracture profiles for broken Charpy specimens at room temperature are shown.

The variation of mechanical properties for the as-hot-rolled steels at different cooling rate are shown in Figs. 27 and 28. The water quenched steel exhibits higher strength than the air cooled steel, due to the incorporation of martensite in the ferrite matrix. However, the air cooled steel shows higher

ductility and impact toughness. The fracture modes of the broken Charpy specimens at different cooling rates are shown in Fig. 30b (water quenching) and Fig. 31 (air cooling). These behaviors presumably result because the ferrite matrix in the water quenched condition is work hardened due to the deformation in the ($\alpha+\gamma$) region followed by fast cooling, while the air cooled specimen contains a recovered ferrite substructure. Also, the higher volume fraction and the higher strength of the second phase in the water quenched specimen (martensite) than in the air cooled specimen (pearlite) might cause in this behavior [40].

Consequently, all of the above observations show the importance of grain size refinement for dual phase steels and indicate that the hot rolling process is a promising method by which a fine grain dual phase structure and desirable mechanical properties can be obtained economically. Moreover, the finishing rolling temperature ($950^{\circ}C-1000^{\circ}C$) for Fe/2Si/0.1C steel is desirable for conventional hot working practice without encountering excessive rolling load. However, in order to apply the hot rolling process to commercial production process, the effects of rolling schedule, soaking temperature still have to be clarified. The general applicability of the results in this investigation must be regarded as preliminary.

IV. Conclusions

Based on the present investigation of the effect of grain size on the mechanical properties of duplex Fe/2Si/0.1 steels, the following conclusions are drawn.

A. Intermediate Quenching Treatment

1. As the prior austenite grains are refined, improvements in total elongation, reduction in area and impact toughness can be achieved, while uniform elongation, yield and tensile strengths are not affected.

2. These improvements in mechanical properties are attributed to the refinement of DFM structural sub-unit.

3. The sub-unit of the DFM structure is the basic microstructural unit controlling the fracture behavior.

4. The sub-unit size of the DFM structure is almost identical to the initial martensite packet size, and can be controlled by the prior austenite grain size.

5. Refinement of the prior austenite grain size does not cause any observable difference in the morphology or substructure of the DFM structure except for a decrease in the size of the sub-unit.

6. Microcracks are initiated near the ferrite-martensite interface, not the martensite particle.

7. At a constant prior austenite grain size, the volume fraction of martensite influences the strength and ductility according to the 'rule of mixtures'. However, the volume fraction of martensite has little effect on the impact toughness and reduction in area.

B. Thermomechanical Treatment

1. The hot rolling process was proved to be an effective way to obtain microduplex structure and attractive mechanical properties.

2. For the water quenched steels, the improvement in ductility and impact toughness was achieved without a sacrifice of tensile strength through hot rolling.

3. For the air cooled condition, the tensile strength of hot rolled alloy was higher than that of non-deformed alloy, without loss in ductility.

4. These improvements in mechanical properties by hot rolling are closely related to the ferrite grain refinement.

5. Finishing rolling temperature in the (α+γ) region has an influence on the mechanical properties. The strength of the water quenched specimen decreases with lower finishing temperature, but increases for the air cooled condition.

6. From a commercial standpoint, Fe/2Si/0.1C alloy is clearly desirable to have duplex structure at finishing rolling temperatures similar to those commonly used in conventional hot working practice.

ACKNOWLEDGEMENTS

REFERENCES

1. Carlo Parrani et al., <u>Micro Alloying 75</u>, Proc. Symposium on High Strength, Low-Alloy Steels, Washington, D. C., October 1-3, 1975. Union Carbide Corporation, N.Y., 1977, p.288.

2. A. T. Davenport, ed., <u>Formable HSLA and Dual-Phase Steels</u>, AIME, New York, N.Y., 1979.

3. R. A. Kot and J.W. Morris, eds., <u>Structure and Properties of Dual-Phase Steels</u>, AIME, Warrendale, PA., 1979.

4. R. A. Kot and B. L. Bramfit, eds., <u>Fundamentals of Dual-Phase Steels</u>, Warrendale, PA., 1981.

5. J. Y. Koo, Ph.D. Thesis, University of California, Berkeley, 1977, (LBL-6657).

6. N. J. Kim and G. Thomas, Met. Trans. <u>12A</u> (1981), p. 483.

7. M. J. Young, M.S. Thesis, University of California, Berkeley 1977, (LBL-6620).

8. T. J. O'Neill, M.S. Thesis, University of California, Berkeley, 1979, (LBL-9047).

9. P. K. Costello, M.S. Thesis, University of California, Berkeley, 1978, (LBL-8628).

10. R. L. Smith, G. Spangler and R. M. Brick, Trans.ASM <u>46</u> (1954), p. 973.

11. K. J. Irvine, <u>JISI</u>, October (1962), p. 820.

12. W. B. Morrison and R. L. Miller, <u>Ultrafine Grain Metals</u>, Proc. 16th Sagamore Conf., p. 183. Syracuse University Press, 1970.

13. R. A. Grange, Trans. ASM <u>59</u> (1966), p. 26.

14. M. J. Roberts, Met. Trans. 1 (1970), p. 3287.

15. H. Ohtani, F. Terasaki and T. Kunitake; Tetsu-to-Hagane 58 (1972), p. 434.

16. T. Swarr and G. Krauss, Met. Trans. 7A (1976), p. 41.

17. T. Inoue, S. Matsuda, Y. Okamura and K. Aoki, Trans. JIM 11 (1970), p. 36.

18. Annual Book of ASTM Standards, Designation E8-69, p. 196 (1973).

19. Ibid., Designation, E23-72, p. 277.

20. J. Y. Koo and G. Thomas, Mat. Sci and Engr. 24 (1976) p. 187.

21. R. A. Grange, Met. Trans. 2 (1971), p. 65.

22. G. Krauss and A. R. Marder, Met. Trans. 2 (1971), p. 2343.

23. S. K. Das and G. Thomas, Met. Trans. 1 (1970), p. 325

24. C. A. Apple, R. N. Caron and G. Krauss, Met. Trans. 5 (1974), p. 593.

25. T. Maki, K. Tsuzaki and I. Tamura, Tetsu-to-Hagane 65 (1979), p. 518.

26. E. E. Underwood, ASM Metals Handbook Vol. 8 (1961), p. 37.

27. B. V. N. Rao, J. Y. Koo and G. Thomas, 33rd Annual Proc. Electron Microscopy Soc. America, Claitors, Baton Rouge (1975), p. 30.

28. J. W. Christian, The Theory of Transformations in Metals and Alloys. Pergamon, N. Y., 1965.

29. K. J. Irvine and F. B. Pickering, J. Iron and Steel Inst. 201 (1963), p. 944.

30. J. Y. Koo, M. J. Young and G. Thomas, Met. Trans. 11A

(1980) p. 852.

31. J. R. Low, Jr., Fracture, B. L. Averbach, D. K. Felback, G. T. Hahn and D. A. Thomas, eds., The M.I.T. Press, Cambridge, Mass. (1959), p. 68.

32. J. H. Bucker, J. D. Grozier and J. F. Enrietto, Fracture (Vol. VI Fracture of Metals), H. Liebowitz, ed., Academic Press, N. Y. (1969), p. 247.

33. G. E. Dieter, Mechanical Metallurgy, 2nd ed. McGraw-Hill (1976) p. 348.

34. Micro-Alloying 75, Union Carbide Corp., N. Y. (1977).

35. P. G. Shewmon, Transformation in Metals, McGraw-Hill (1969).

36. H. I. Aaronson, H. A. Domian and G. M. Pound, Trans. AIME 236 (1966), p. 753.

37. E. O. Hall, Proc. Phys. Soc. London, B64 (1951), p. 747.

38. N. J. Petch, J. Iron and Steel Inst. 174 (1953), p. 25.

39. T. Tanaka, N. Tabata, T. Hatomura and C. Shiga, Micro-Alloying 75, Union Carbide Corp., N. Y. (1977) p. 107.

40. N. J. Kim, Ph.D. Thesis, University of California, Berkeley 1981 (LBL-12661).

TABLE 1. Tensile Properties After Intermediate Quenching Treatment

Specimen	Heat Treatment	Two Phase Annealing Temp.	Vm(%)	Y.S. (ksi)	Y.S. (MPa)	U.T.S. (ksi)	U.T.S. (MPa)	e_u(%)	e_T(%)	R.A.(%)
A1	A + T	885°C	∿30	76.1	525.1	135	931.5	16.4	23	34
B1	A + B + T	885°C	∿30	76.0	524.4	133	917.7	16.5	27	49
A2	A + T	910°C	∿45	78.3	540.3	143.9	992.9	14.9	21.6	34
B2	A + B + T	910°C	∿45	78.0	538.2	143.2	988.1	15.1	25.5	47

A - Austenitization at 1100°C for 1 hour, water quenching

B - Austenitization at 1000°C for 8 minutes, water quenching

T - Two-phase annealing for 10 minutes, water quenching.

TABLE II. Charpy Impact Properties After
Intermediate Quenching Treatment (ft-lb)

Specimen	Vm(%)	Testing Temperature (°C)				
		-50	-25	0	25	50
A1	∿30	6.3	7.5	9.2	11.3	17
B1	∿30	7.0	9.2	11.0	15.3	38.3
A2	∿45	6.7	7.7	9.2	11.8	22.7
B2	∿45	9.1	11.2	12.9	16.6	40.1

TABLE III. Microstructural Size

Specimen	Prior Austenite Grain, μm	Martensite Packet, μm	Sub-unit of DFM, μm	Quasicleavage Facet, μm
A1,A2	∿200	∿80	∿77	∿70
B1,B2	∿60	∿30	∿28	∿35

TABLE IV. Tensile Properties After Thermomechanical Treatment

Specimen	Heat Treatment	Two Phase Annealing Temp.	Y.S.		U.T.S.		e_T(%)	e_u(%)
			(ksi)	(MPa)	(ksi)	(MPa)		
S1	AT + WQ	950°C	72.1	497.5	120.4	830.8	16.4	11.0
H1	ATR + WQ	950°C	69.5	479.2	117.0	807.3	25.9	15.5
H2	ATR + WQ	1000°C	73.0	503.7	124.5	859.0	22.5	12.4
S2	AT + AC	950°C	50.0	345.0	77.4	534.0	31.0	18.7
H3	ATR + AC	950°C	65.1	449.0	90.1	621.0	31.2	16.5
H4	ATR + AC	1000°C	61.9	427.1	87.0	600.3	30.0	14.9

AT - Austenitizing at 1150°C for 30 minutes followed by two phase annealing for 10 minutes.

ATR- Austenitizing at 1150°C for 30 minutes followed by hot rolling, and two phase annealing for ten minutes, followed by hot rolling.

WQ - Water quenching.

AC - Air cooling.

TABLE V. Charpy Impact Properties After
Thermomechanical Treatment (ft-lbs)

Specimen	Testing Temperature (°C)				
	-75	-50	-25	0	25
S1	--	5.8	6.5	7.0	9.6
H1	--	7.5	9.4	17.0	50.8
H3	11.2	22.1	59.2	86.5	102.5

FIGURE CAPTIONS

Fig. 1. Schematic of the intermediate quenching heat treatment in

conjunction with the Fe-rich portion of Fe-C phase diagram.

(A) Single austenitizing treatment.

(B) Double austenitizing treatment for grain

refinement.

Fig. 2. Schematic drawing of ASTM specifications for test specimens.

(A) Round tensile specimen.

(B) Standard V-notch impact specimen.

Fig. 3. Optical micrographs of the initial martensite structure before

two phase annealing.

(a) Specimen A1.

(b) Specimen B1.

Fig. 4. Optical micrographs showing the prior austenite grain size

before two phase annealing.

(a) Specimen A1.

(b) Specimen B1.

Fig. 5. Scanning electron micrographs of DFM structure.

(a) Specimen A1.

(b) Specimen B1.

Fig. 6. Transmission electron micrograph of initial martensitic

structure before two phase annealing for specimen A1.

Fig. 7. TEM micrographs revealing the interlath retained austenite in

the 100% martensite structure of specimen A2.

(a) Bright field image.

(b) Corresponding dark field where thin films of

retained austenite reversed contrast when (002)

spot was imaged.

(c) Selected area diffraction pattern.

(d) Indexing of the diffraction pattern in (c), showing

K-S relationship of martensite and austenite.

Fig. 8. TEM micrograph showing martensite and dislocated ferrite in

DFM structure of specimen A1.

Fig. 9. Tensile properties as a function of the austenite grain size

for the DFM steels containing 30% martensite.

Fig.10. Tensile properties as a function of the prior austenite grain

size for the DFM steels containing 45% martensite.

Fig.11. Variation in the Charpy impact energy at different testing

temperatures for the DFM steels containing 30% martensite.

Fig.12. Variation in the Charpy impact energy at different testing

temperatures for the DFM steels containing 45% martensite.

Fig.13. Scanning electron micrographs of tensile fracture surfaces.

(a) Specimen A1.

(b) Specimen B1.

Fig.14. Scanning electron fractographs of broken Charpy impact

specimens tested at $0^{o}C$.

(a) Specimen A2.

(b) Specimen B2.

Fig.15. High magnification scanning electron fractographs of broken

impact specimens tested at $0^{o}C$

(a) Specimen A2.

(b) Specimen B2.

Fig.16. Scanning electron fractographs of broken Charpy impact

specimens tested at $50^{o}C$.

(b) Specimen H1 (Hot rolled).

Fig.31.SEM fractograph of broken Charpy impact specimen (H3) tested at 25°C (hot rolled and air cooled condition)

Fig.32.Microcracks found below the main crack front of broken impact specimen tested at 25°C.

(a) Specimen S1.

(b) Specimen H1.

Fig.33 SEM micrographs of fracture profile of broken impact specimen tested at 25°C.

(a) Specimen S1.
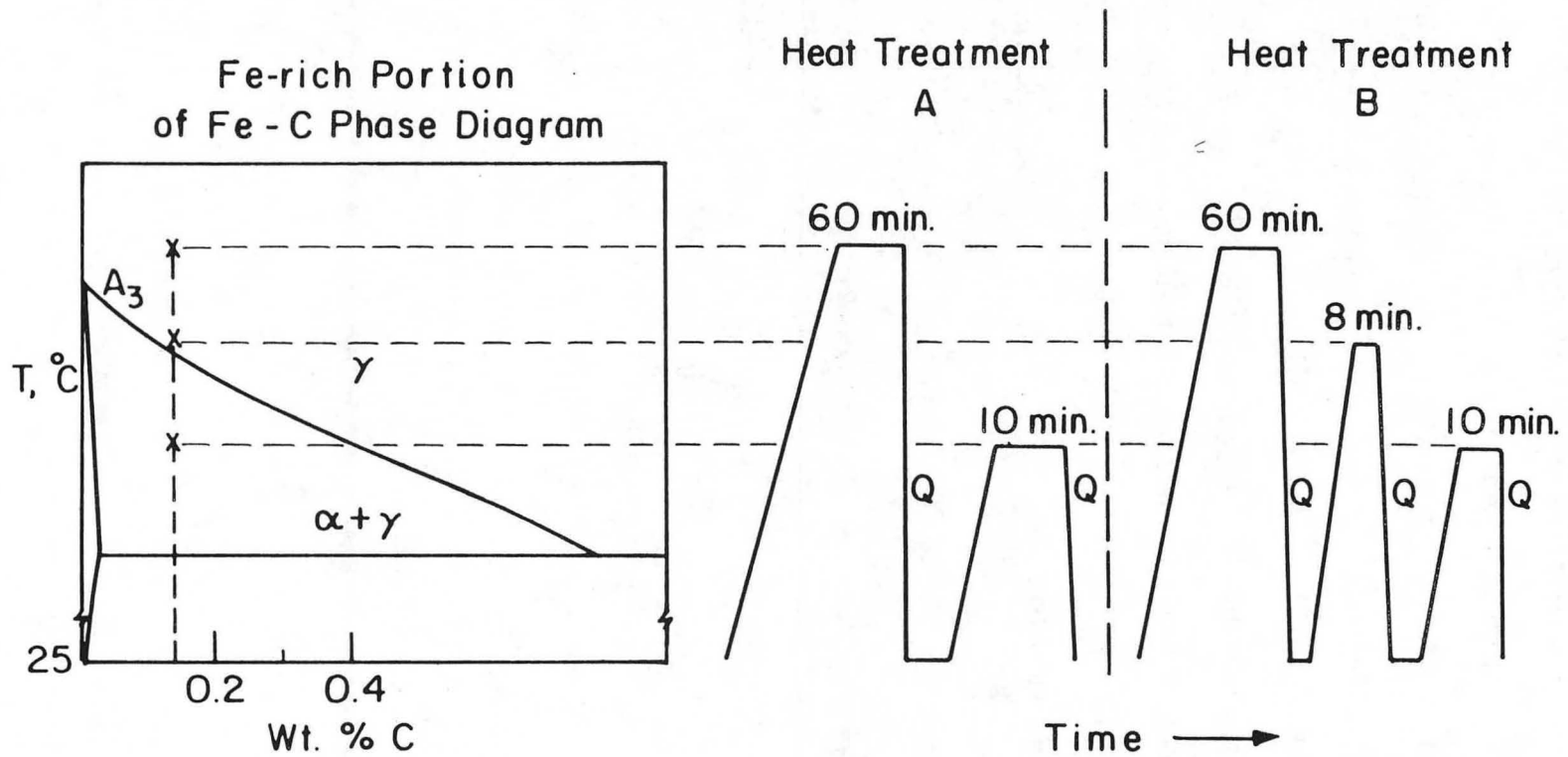
(b) Specimen H1.

Fig. 1

XBL 802-4721
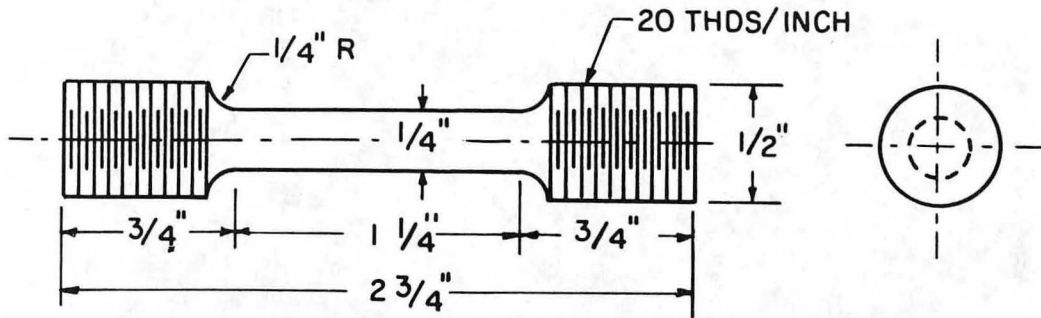
A. ROUND TENSILE SPECIMEN
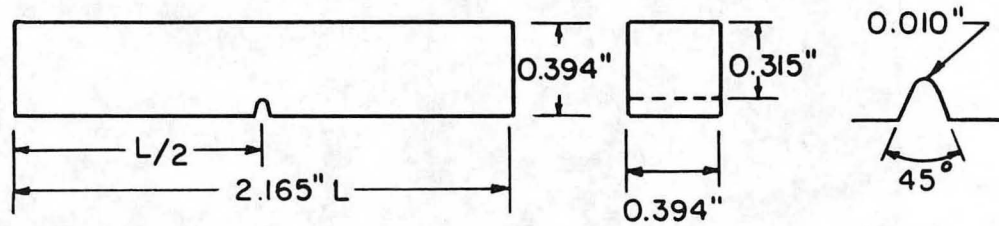
B. CHARPY V-NOTCH IMPACT SPECIMEN

XBL 754-6176

Fig. 2

Fig. 3

200 μ

200 μ

XBB 802-2301

Fig. 4

a 20KU 406X 24.6µ 0002

b 20KU 394X 25.4µ 0001
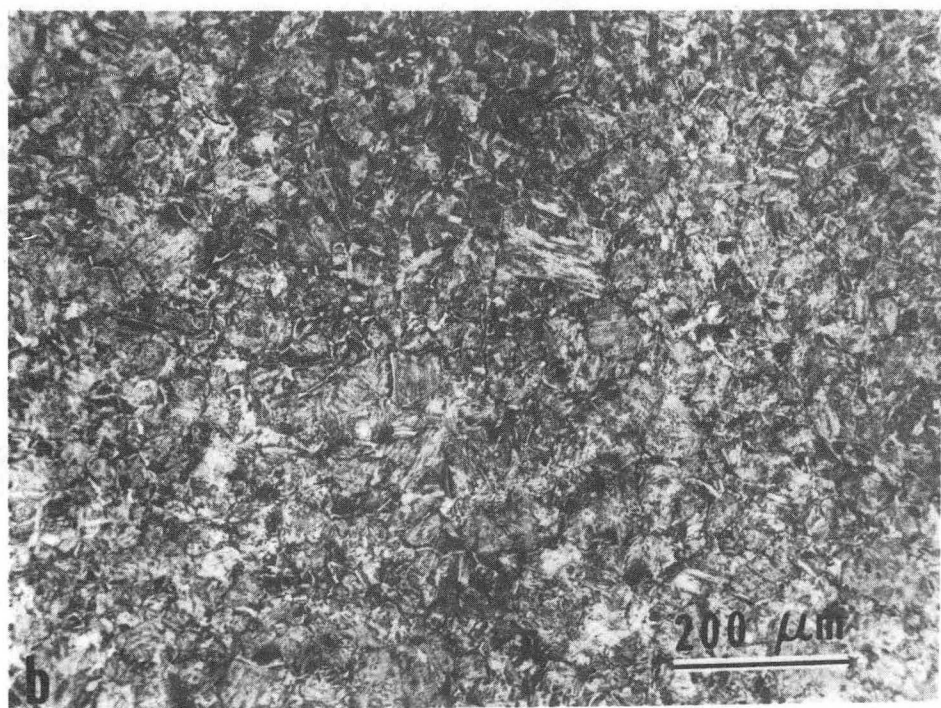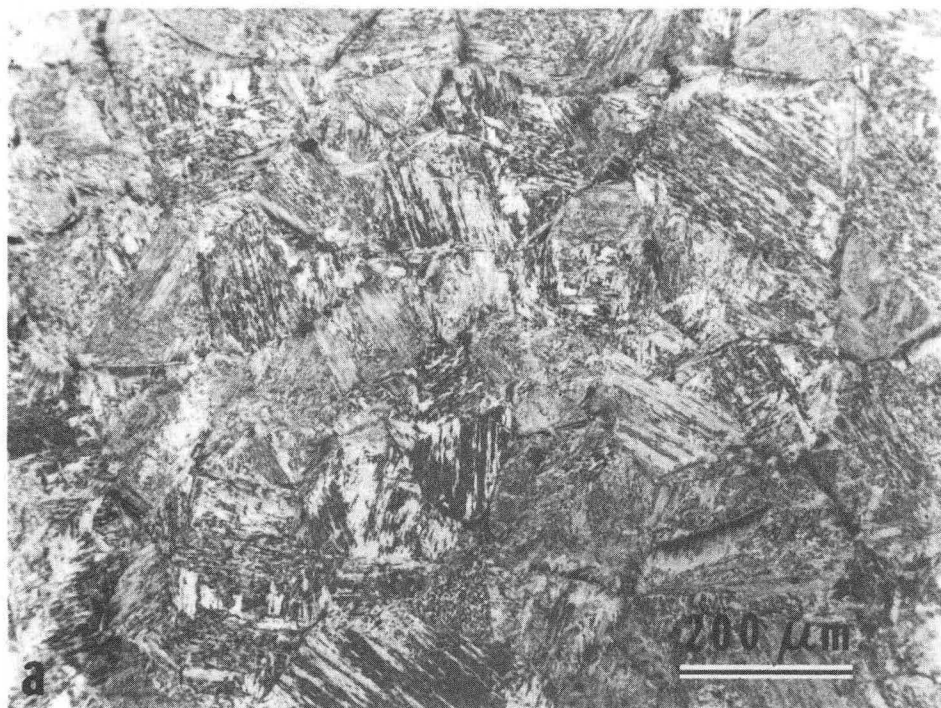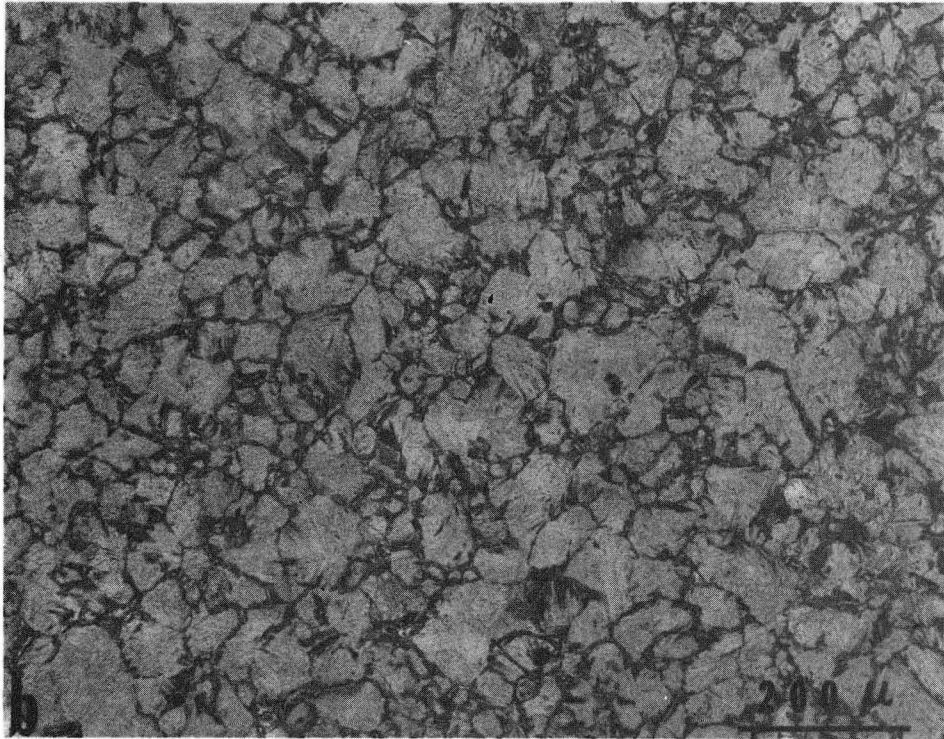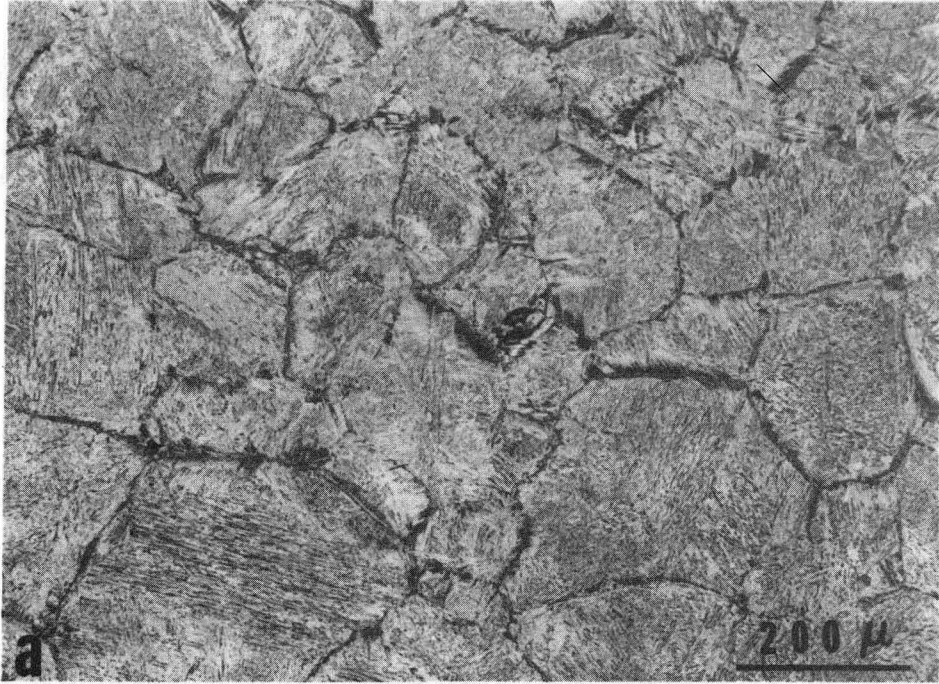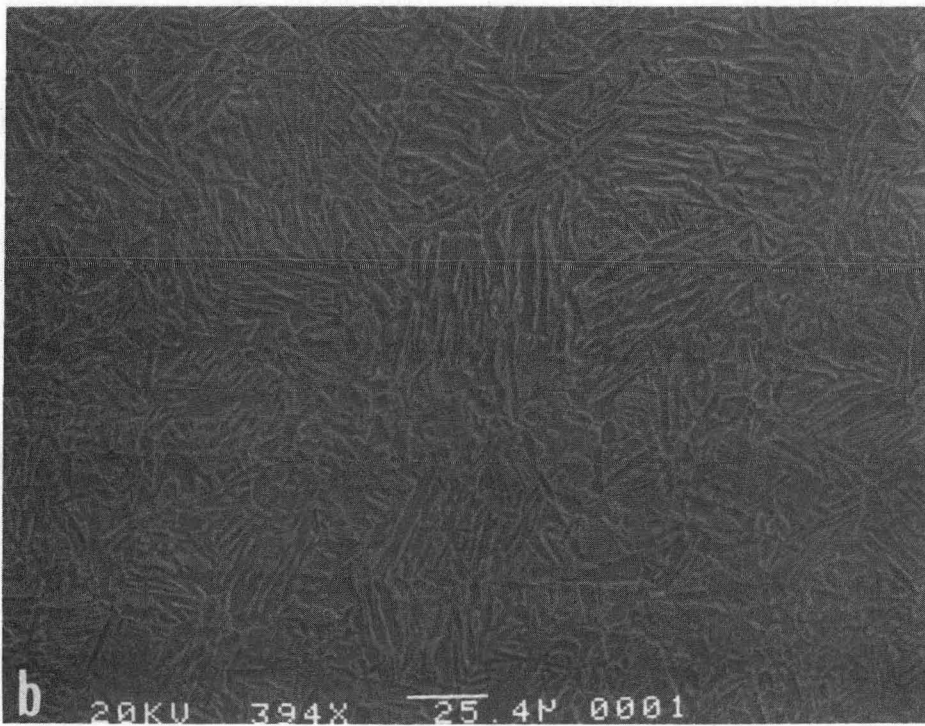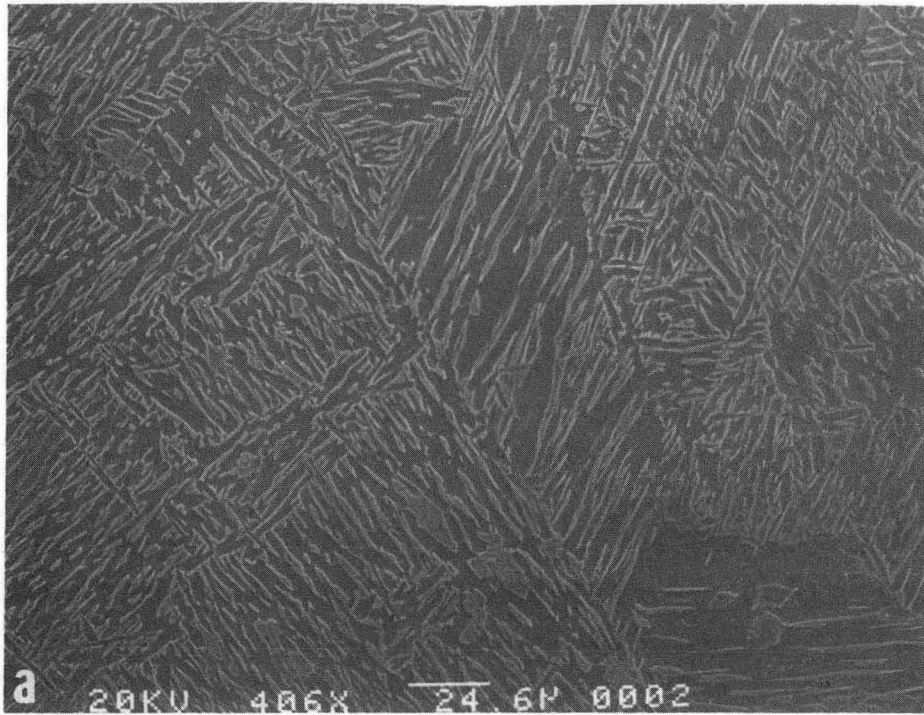
XBB 837-6252

Fig. 5

XBB 837-6267

Fig. 6
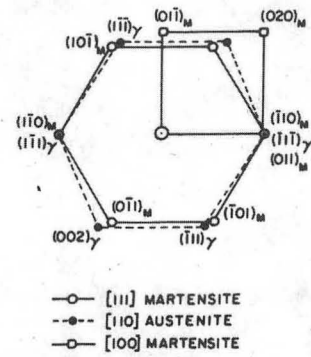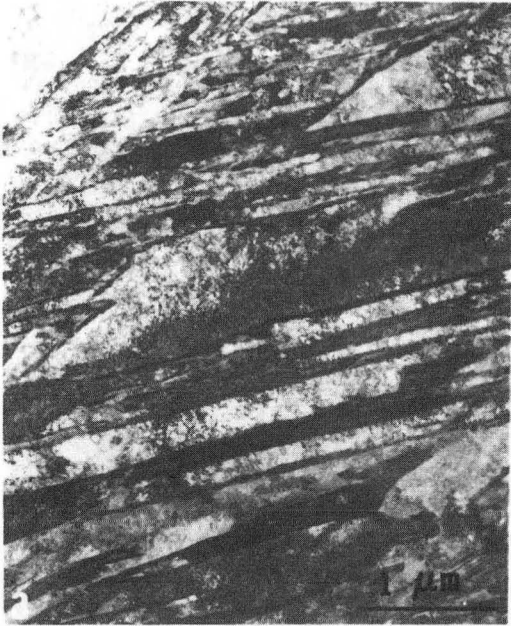
XBB 837-6535

Fig. 7
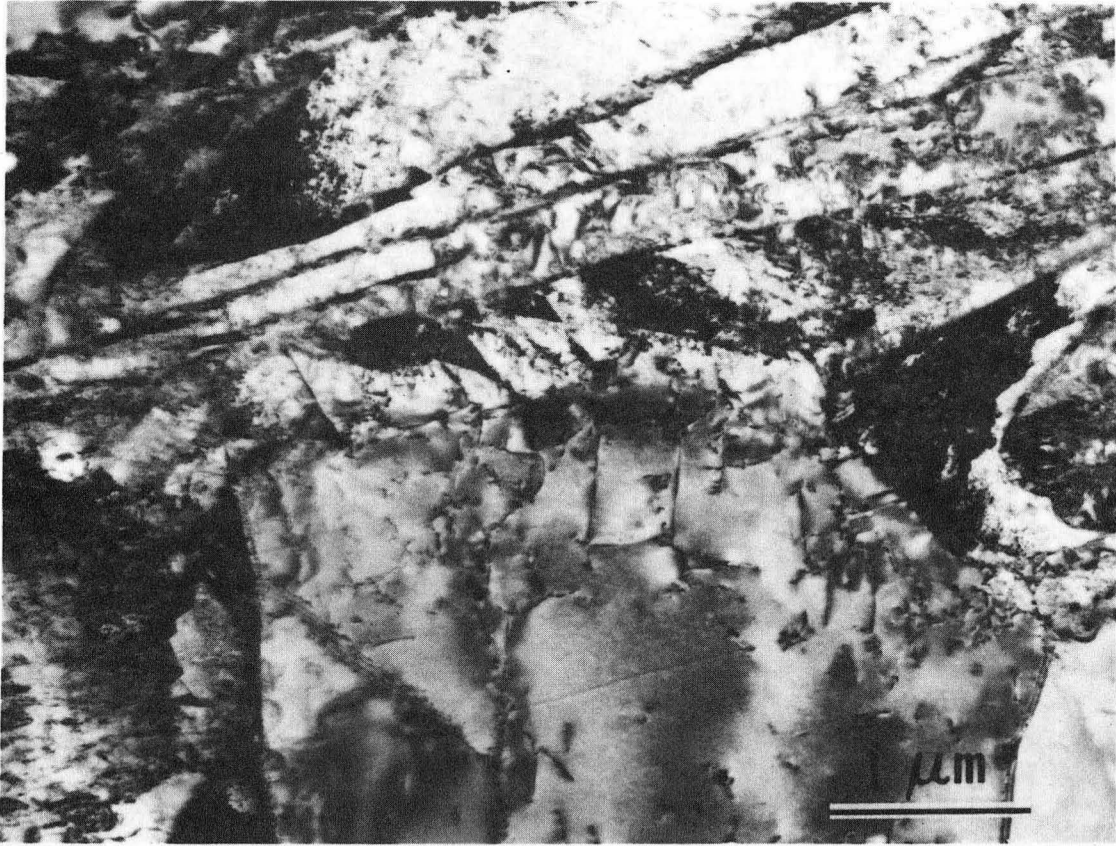
XBB 837-6268

Fig. 8
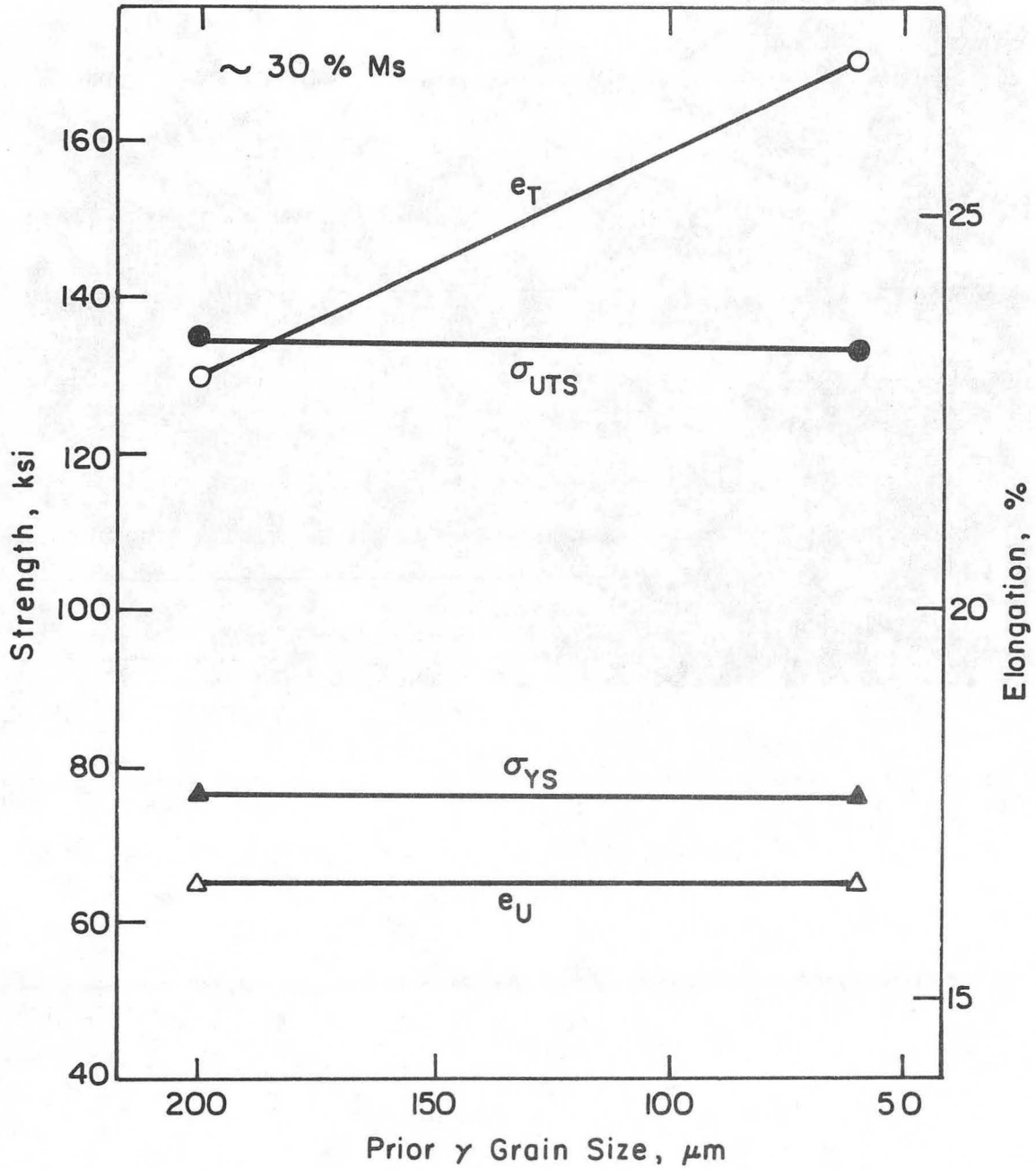
XBL 837-6011

Fig. 9
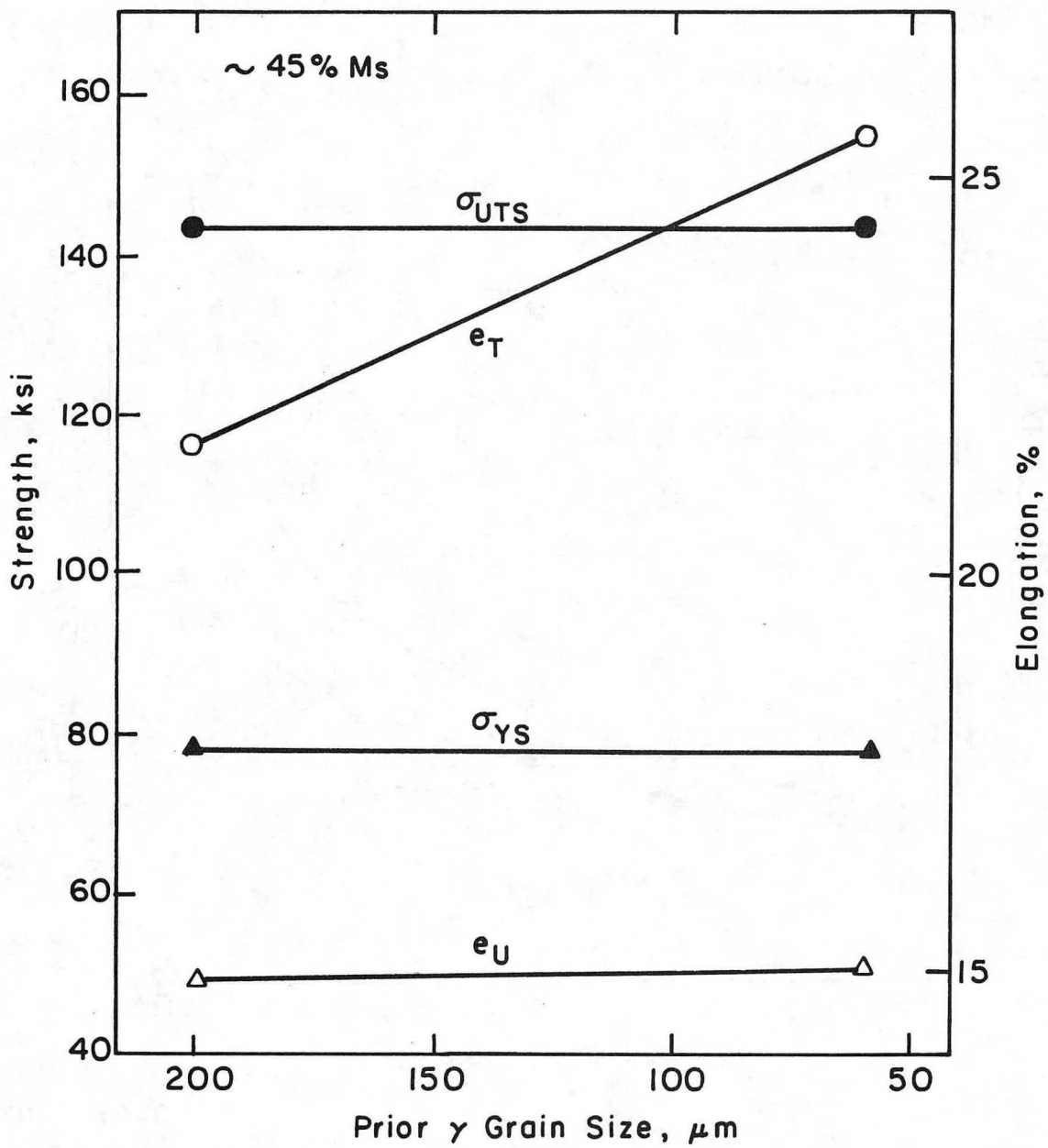
XBL 837-6012

Fig. 10
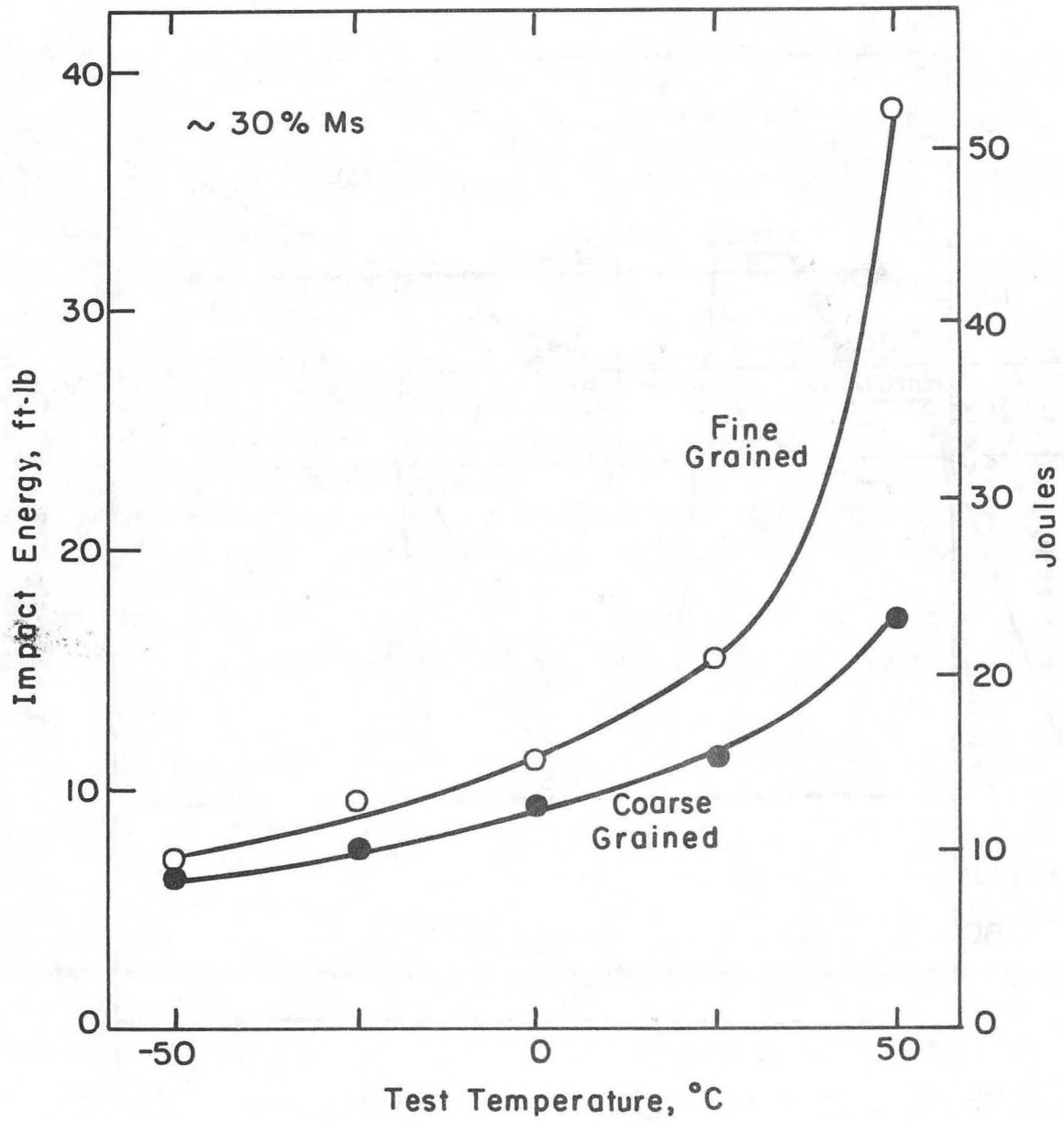
~ 30 % Ms

Fine Grained

Coarse Grained

Impact Energy, ft-lb

Joules

Test Temperature, °C

XBL 837-6013

Fig. 11

Fig. 12

25KV   461X   21.7M 0002

25KV   449X   22.3M 0007

XBB 838-7139

Fig. 13

a 25KU 244X 41.0M 0001

b 25KU 244X 41.0M 0004
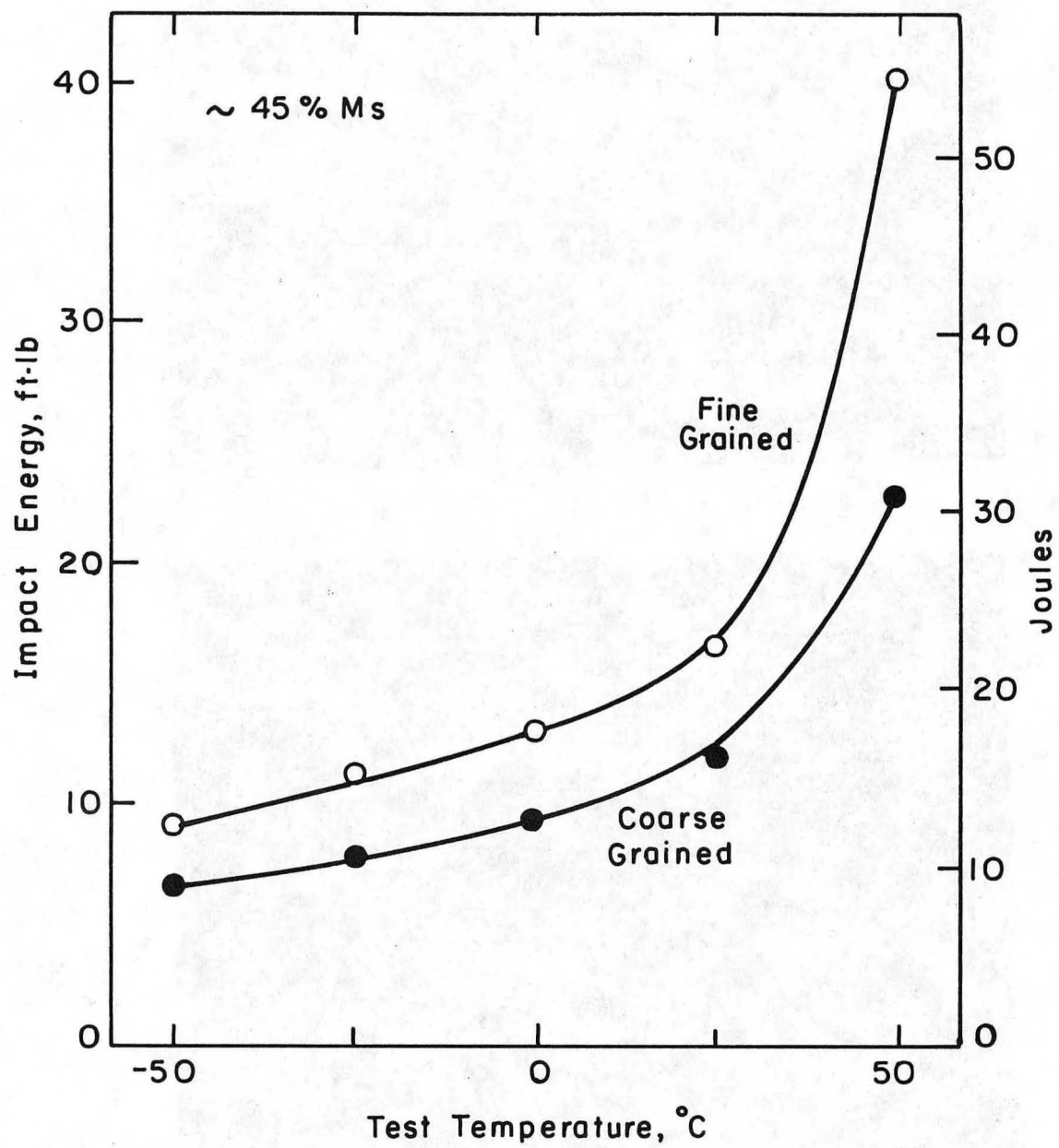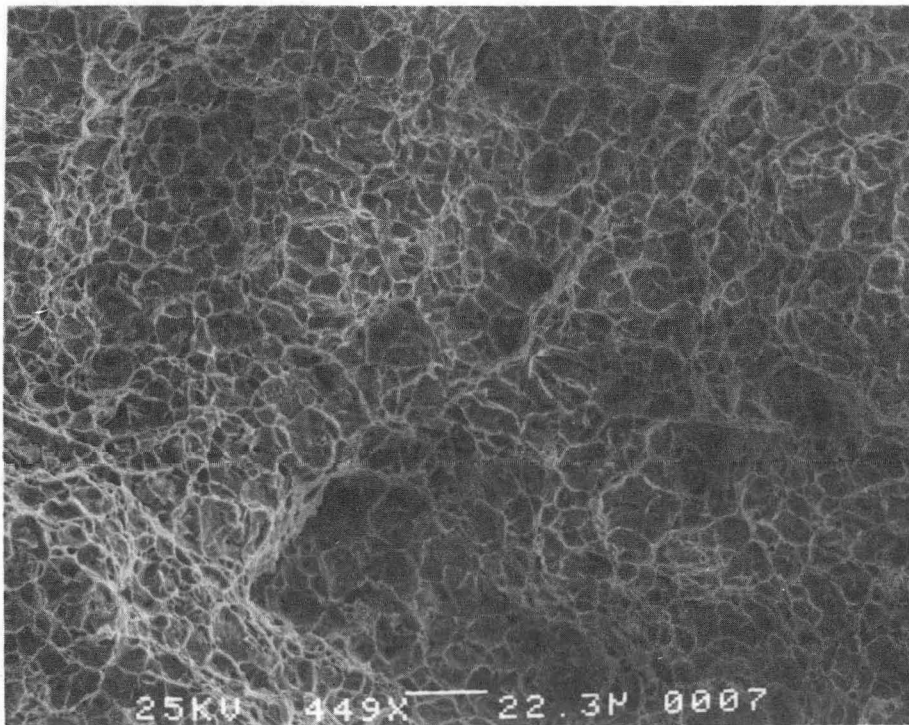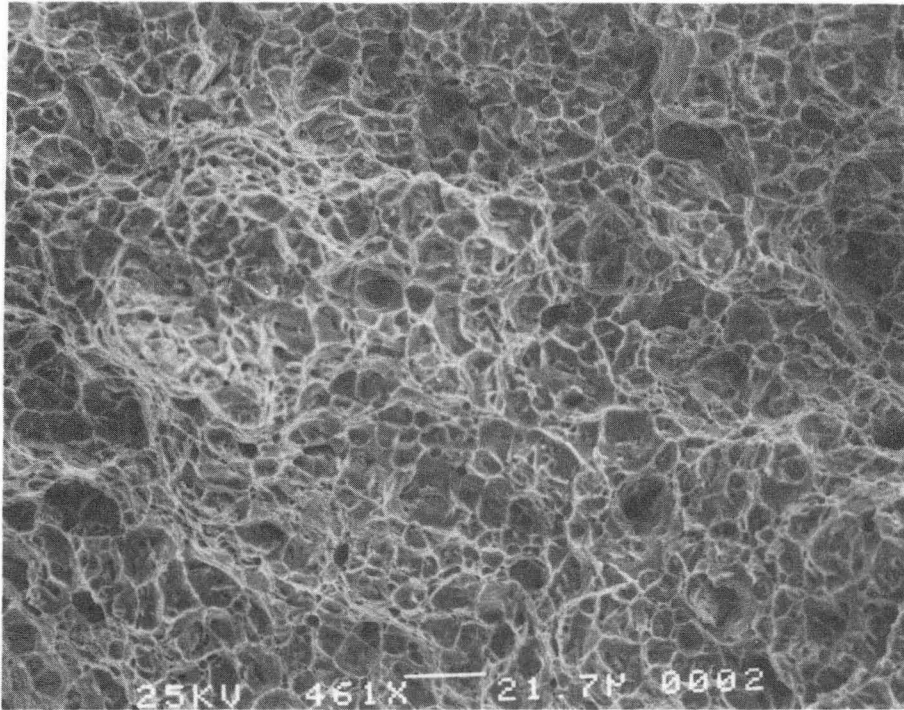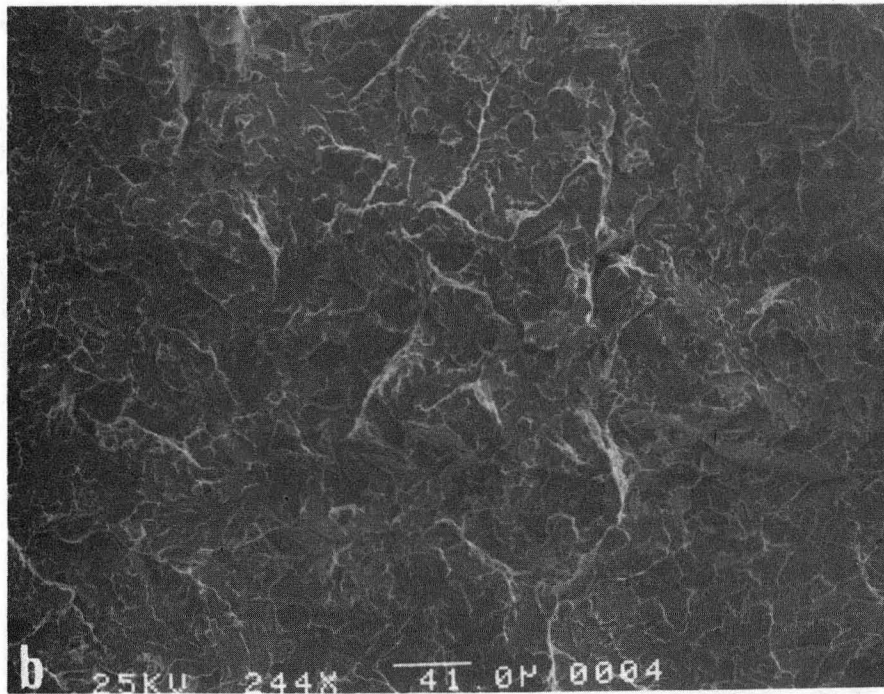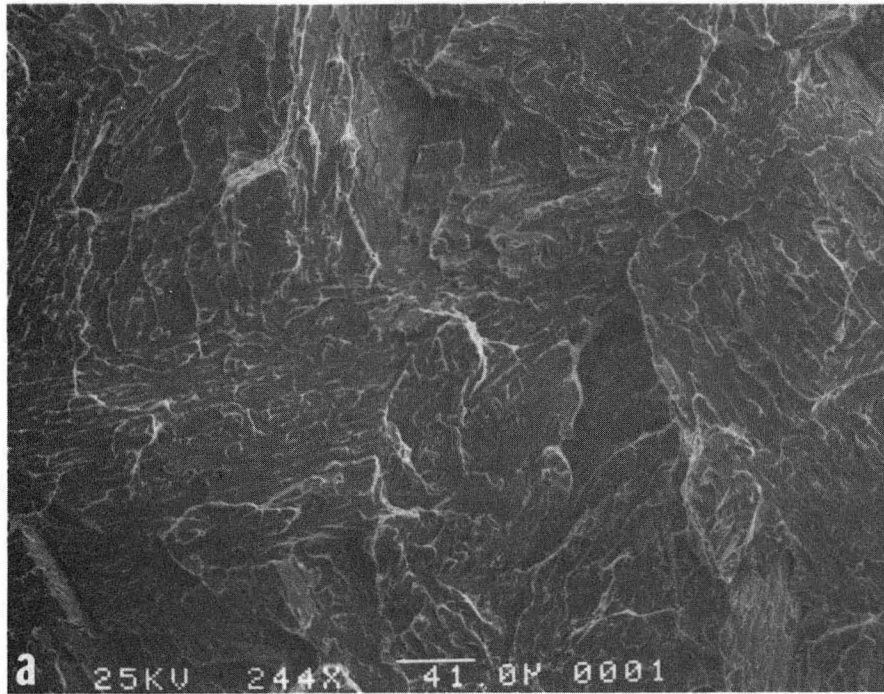
XBB 837-6254

Fig. 14
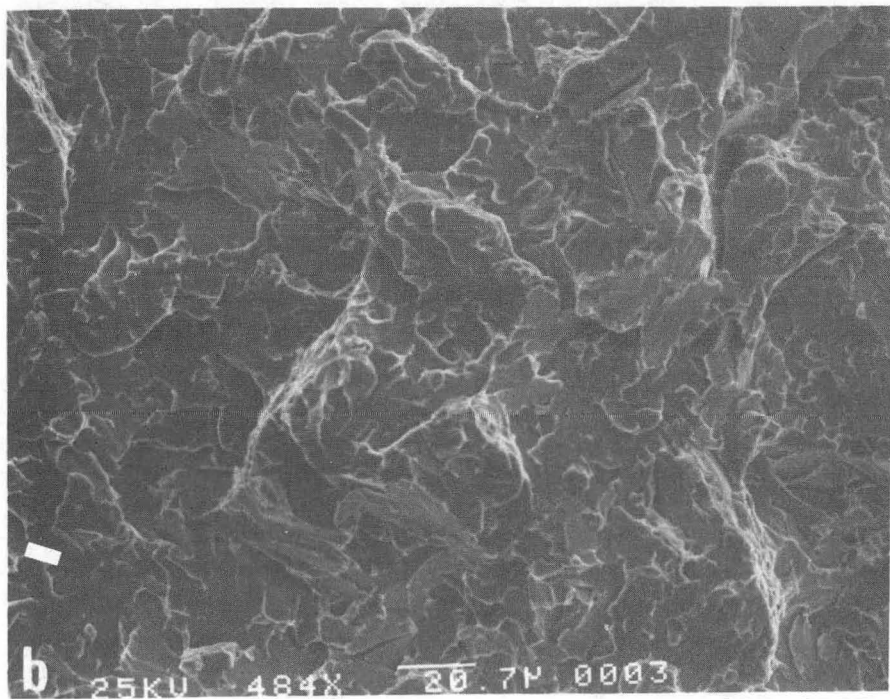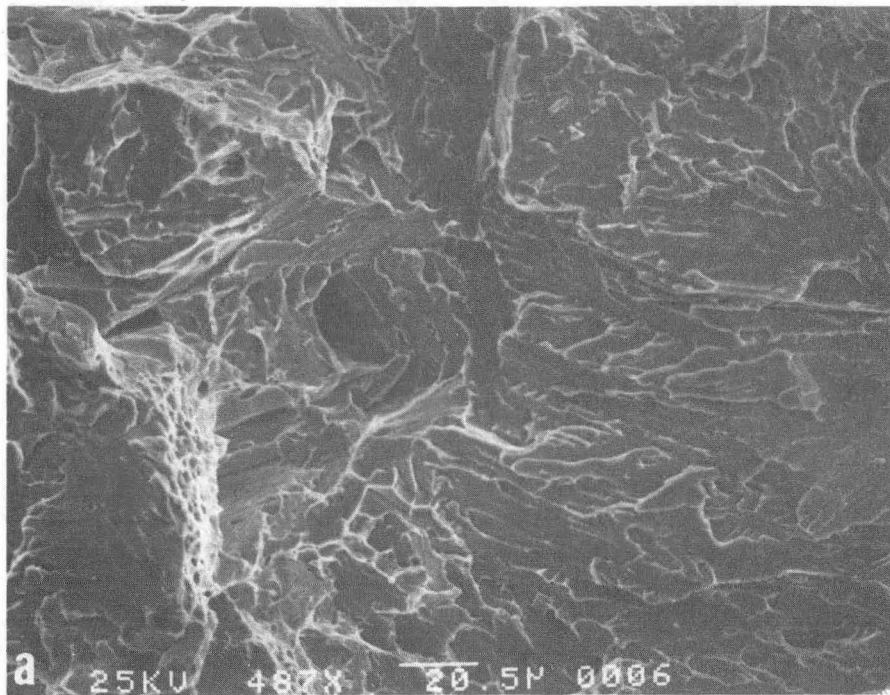
Fig. 15

XBB 837-6256

Fig. 16

50 μm

10 μm

b
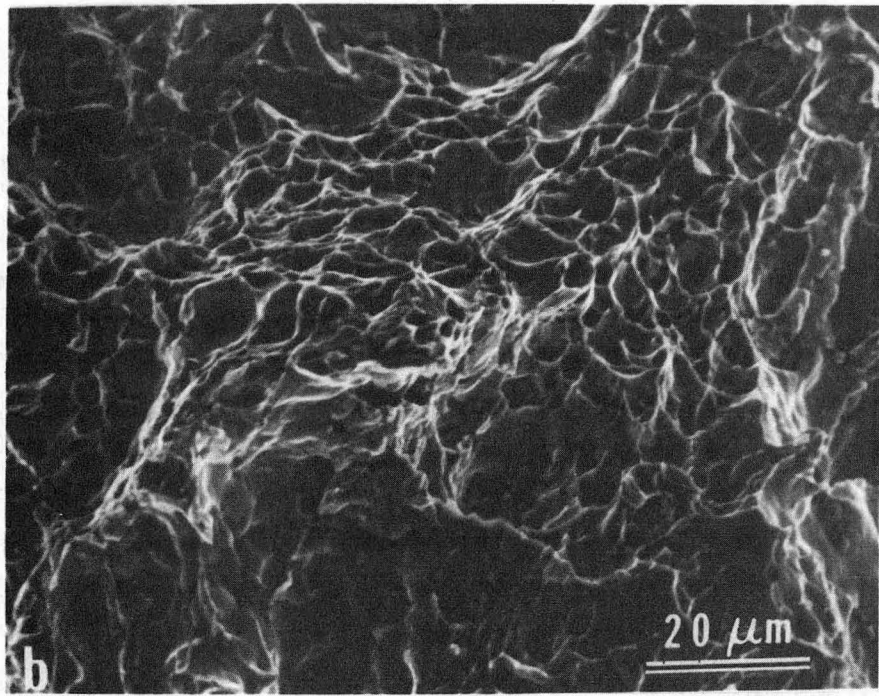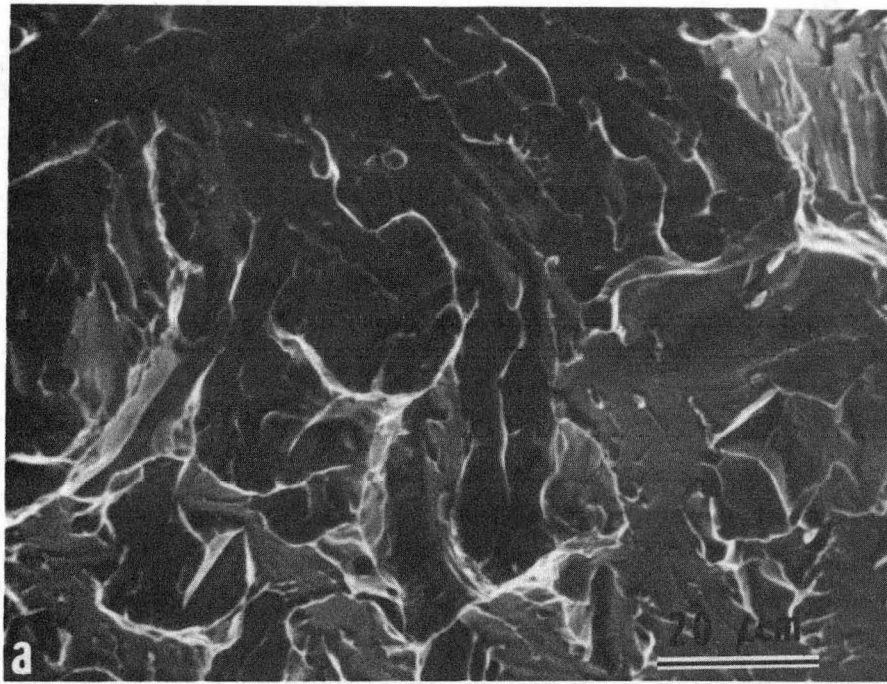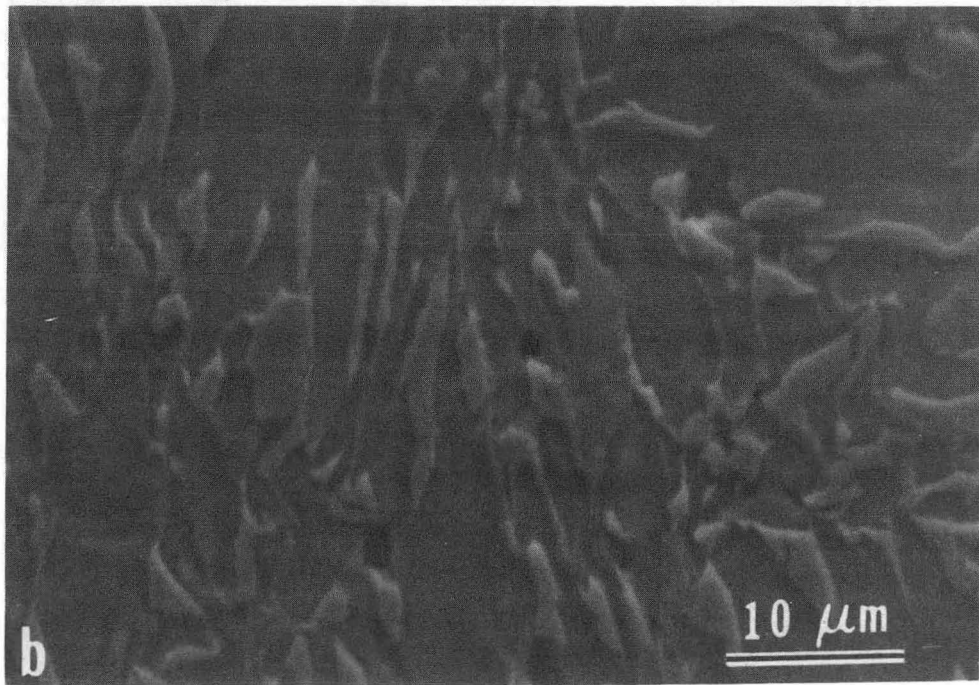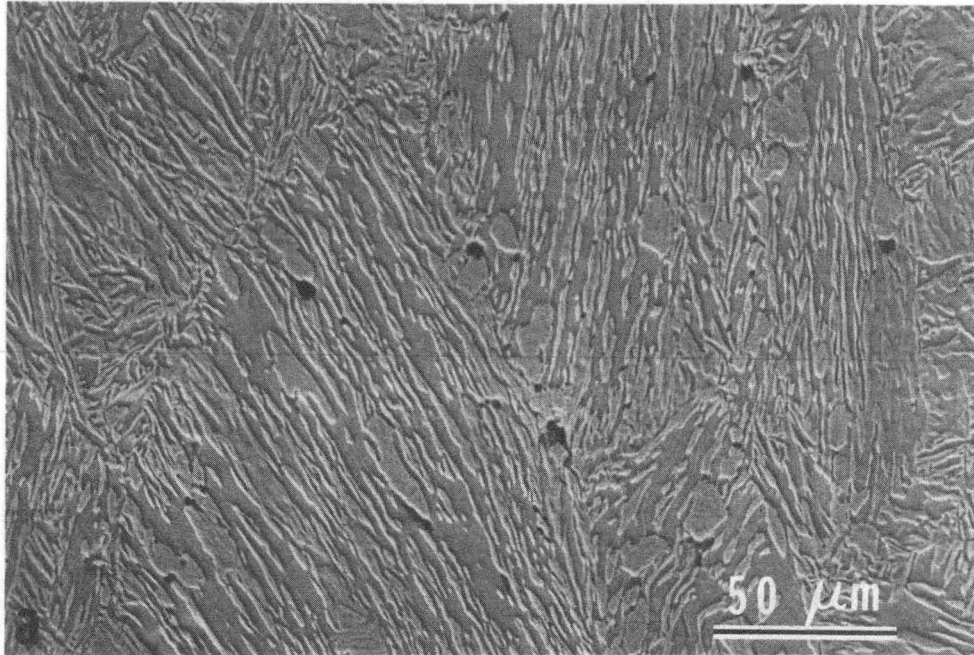
XBB 837-6264

Fig. 17
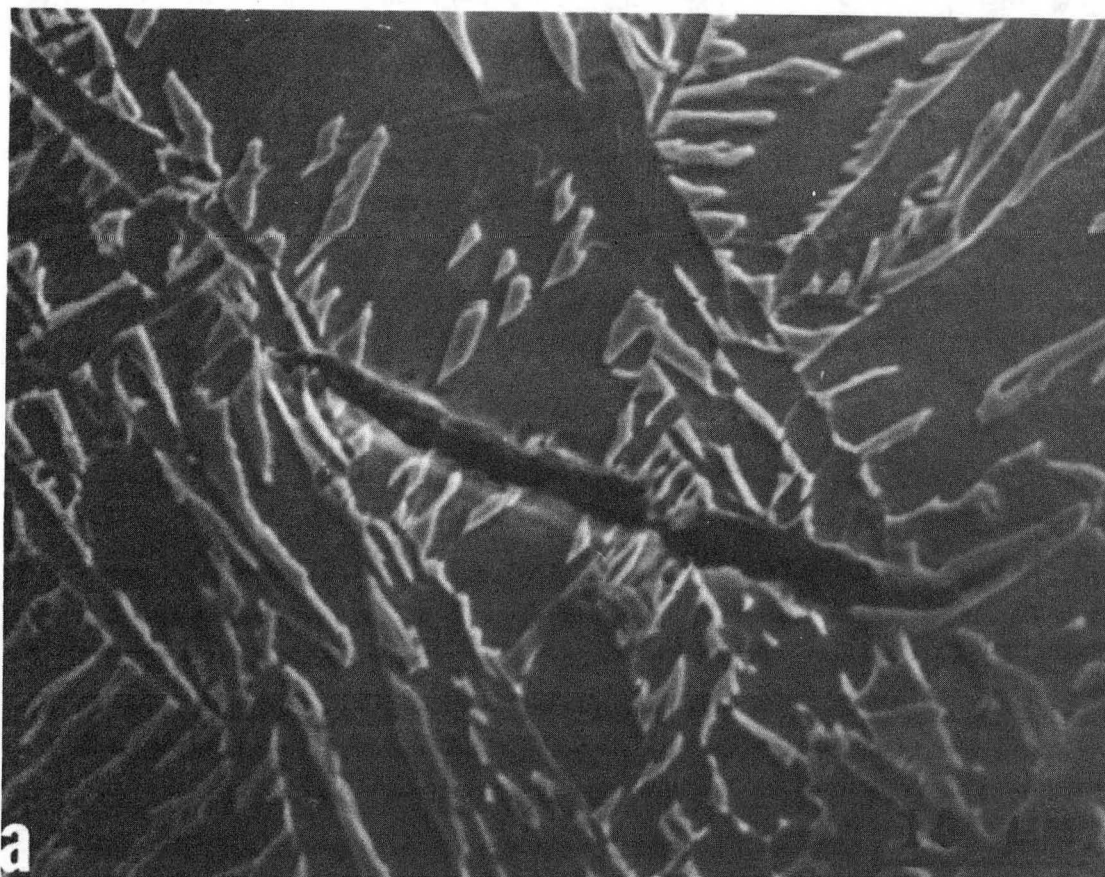
XBB 837-6266

Fig. 18
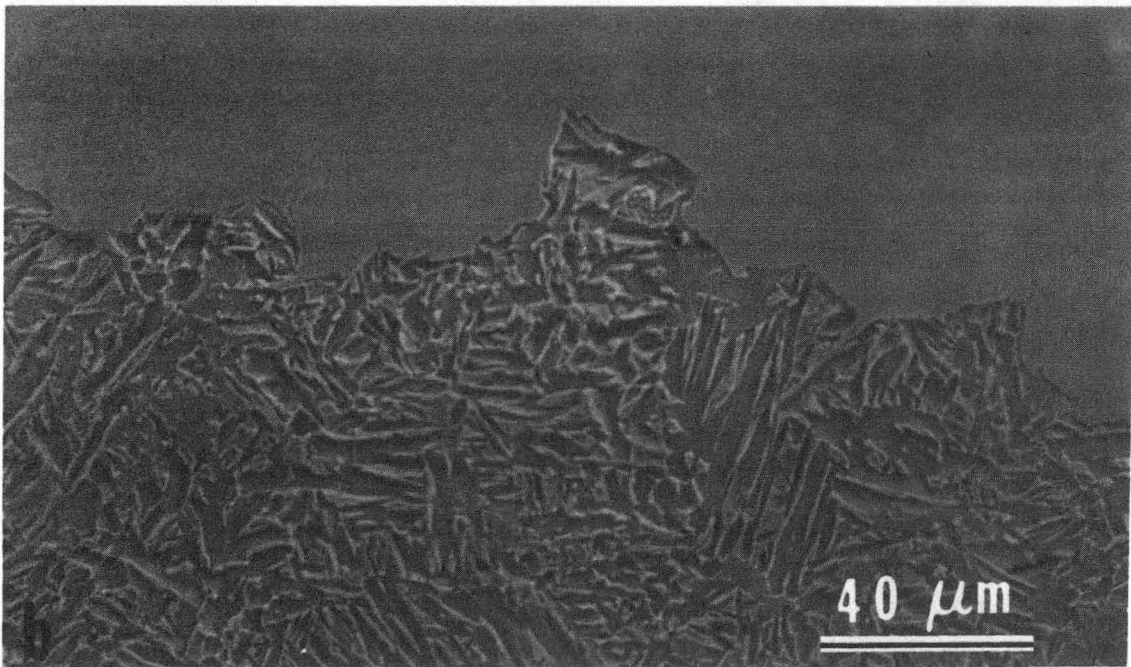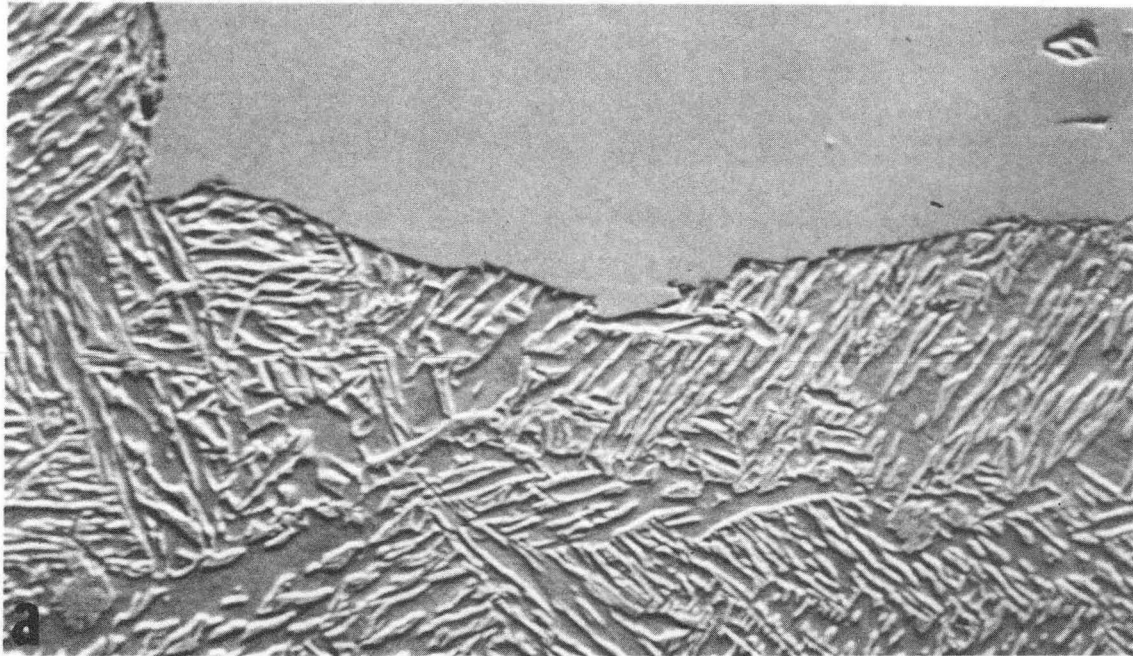
XBB 837-6265

Fig. 19
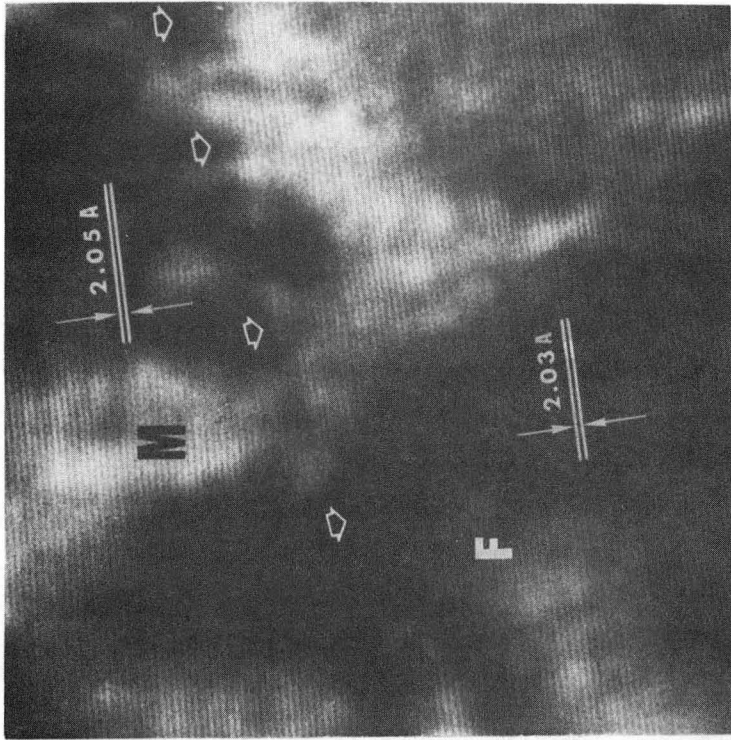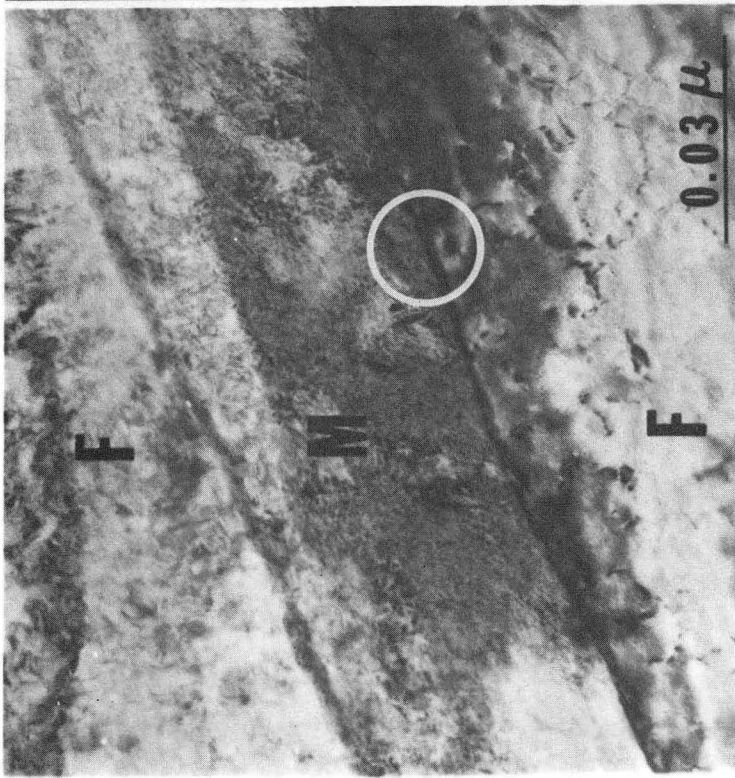
Fig. 20
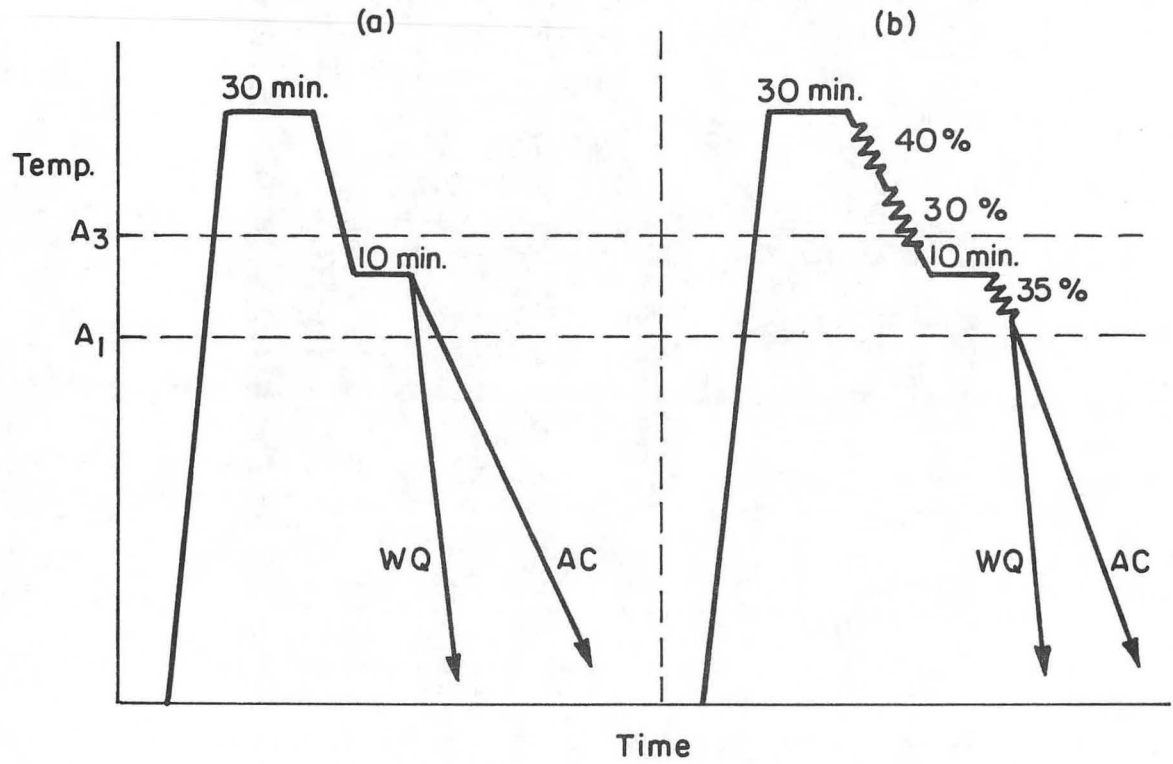
Fig. 21
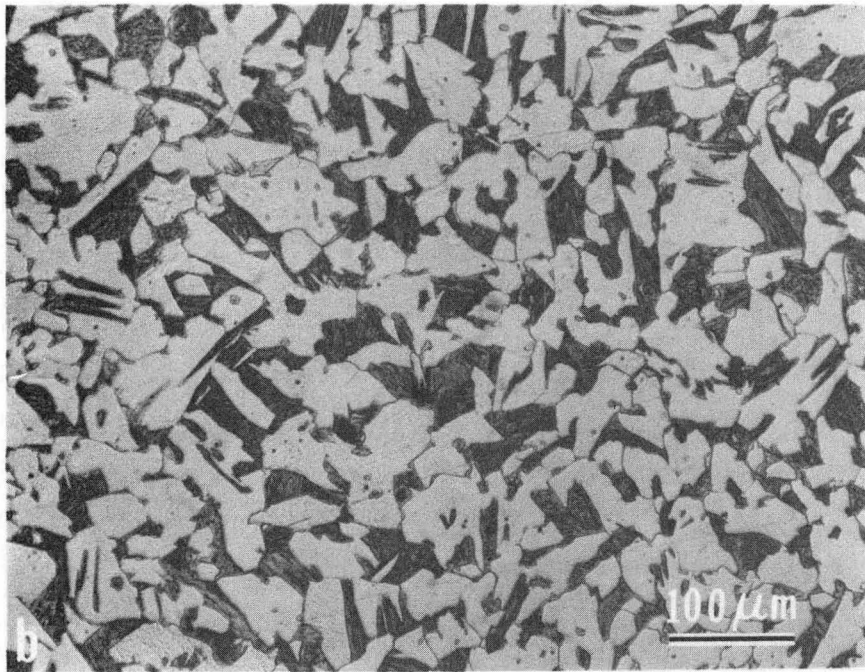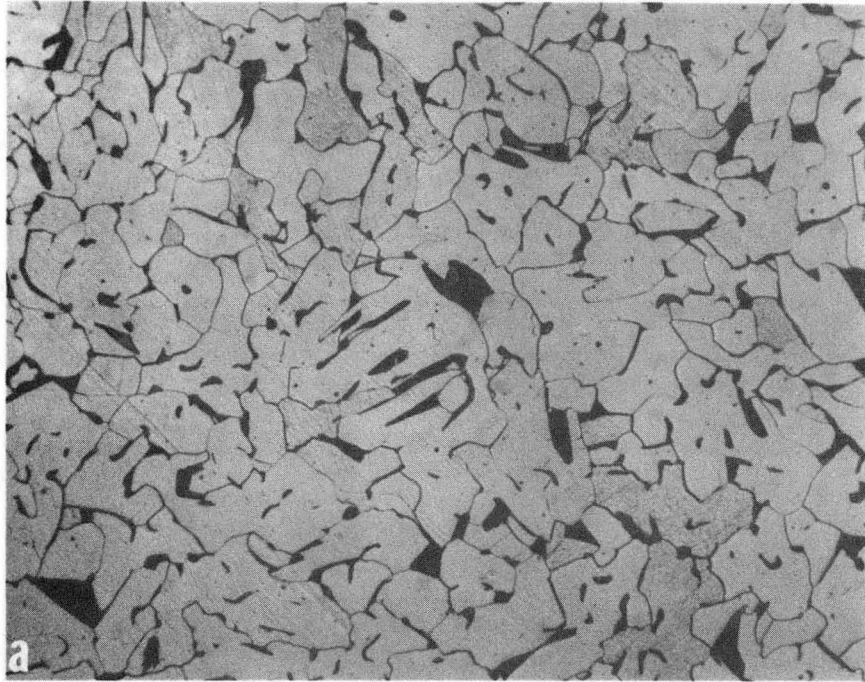
XBL 837-6017

XBB 837-6257

Fig. 22
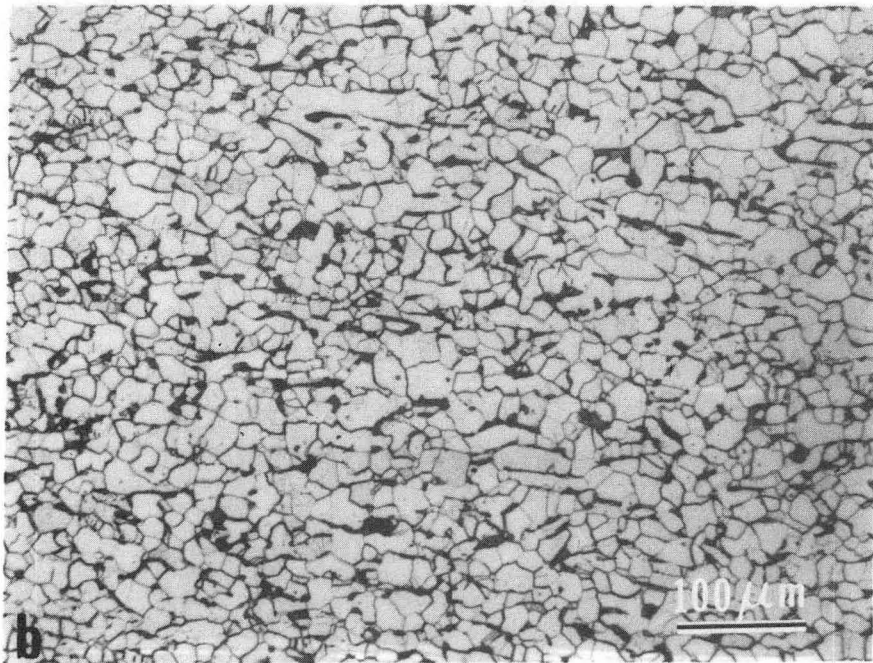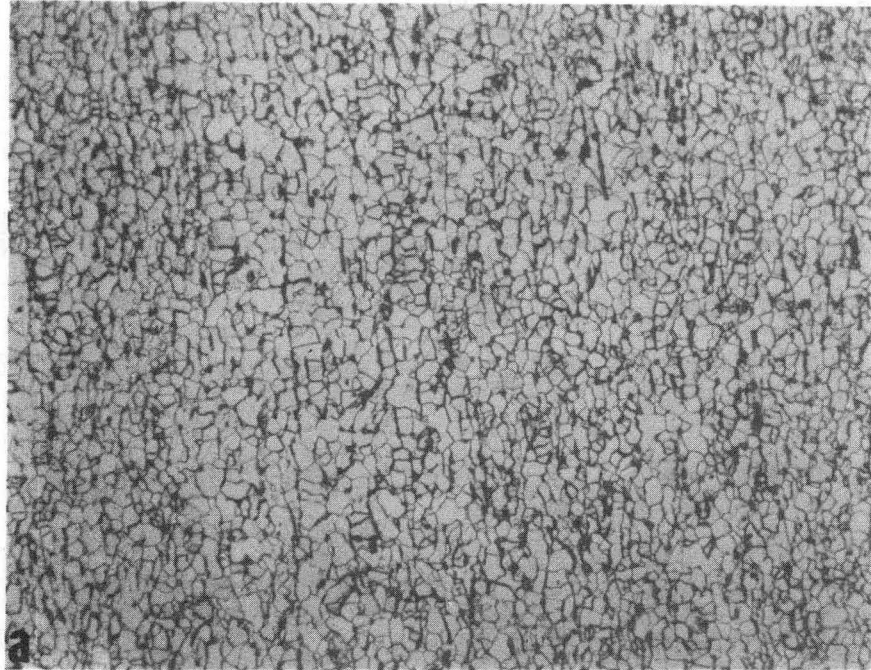
XBB 837-6258

Fig. 23

XBB 837-6259

Fig. 24

1 μm

1 μm

XBB 837-6622

Fig. 25

a

0.5 μm

b

1 μm

XBB 837-6533

Fig. 26

MPa

Step Annealed, Air Cooled
Hot Rolled, Air Cooled
Hot Rolled, Water Quenched
Step Annealed, Water Quenched

Ultimate Strength, ksi
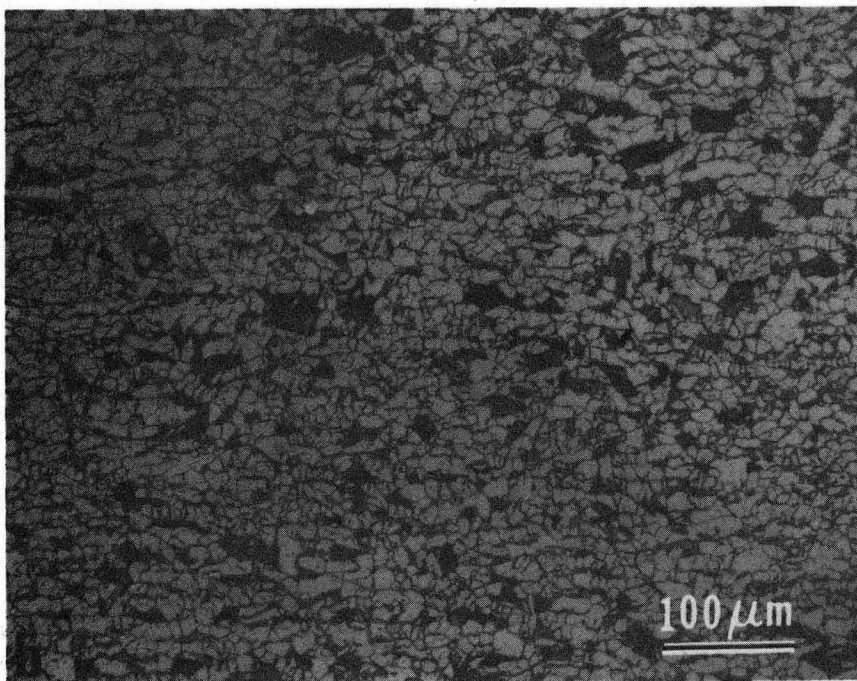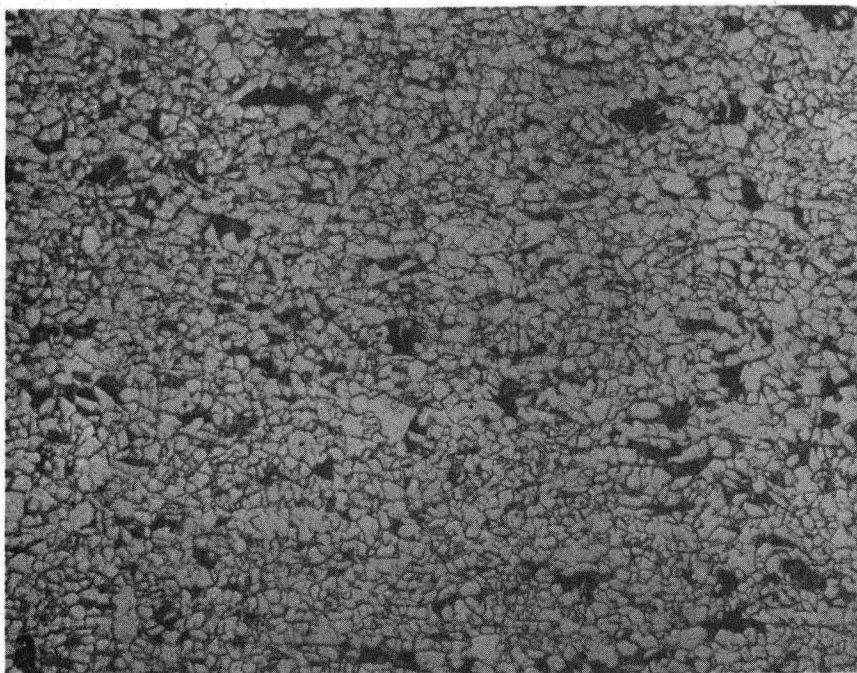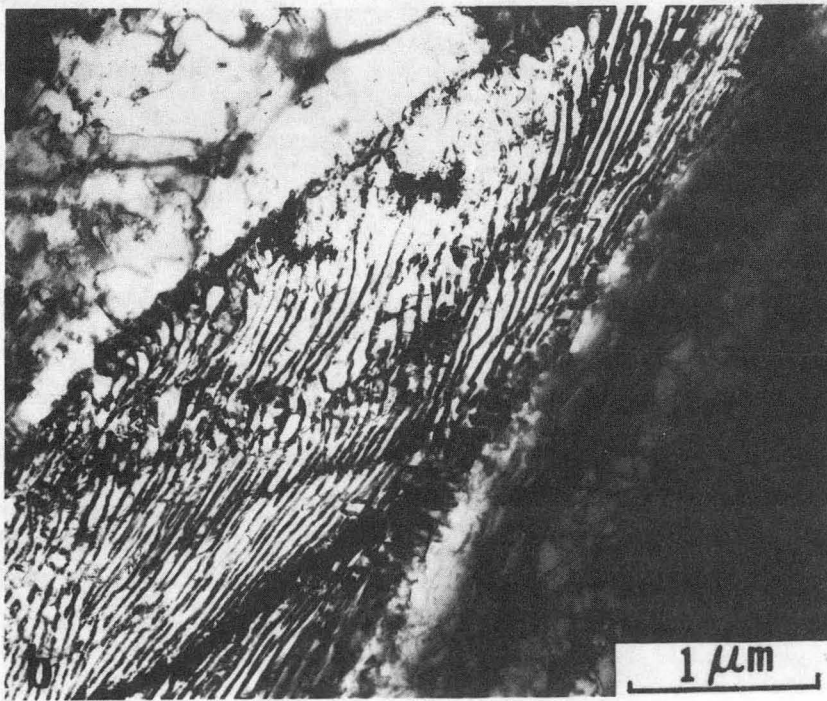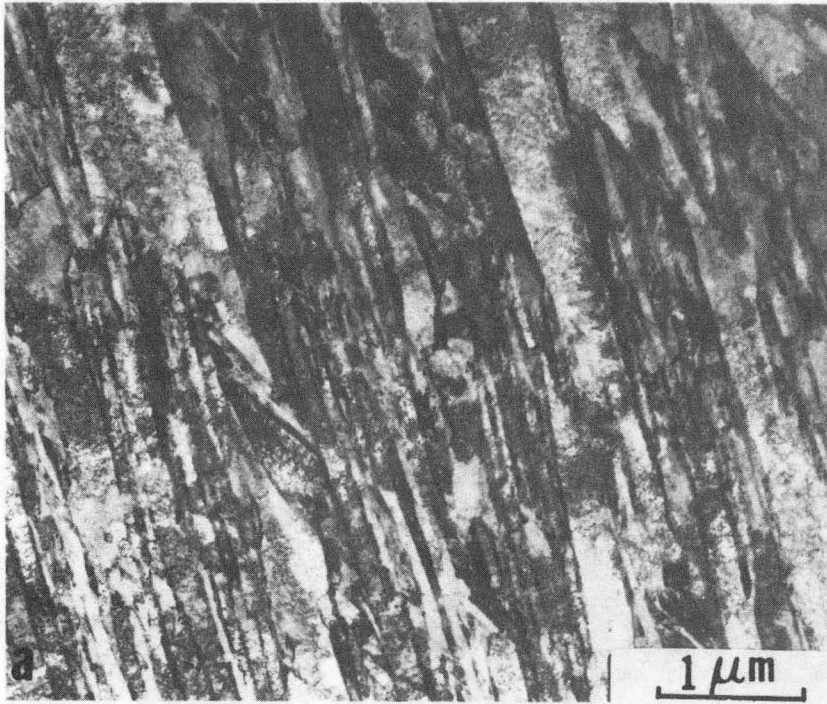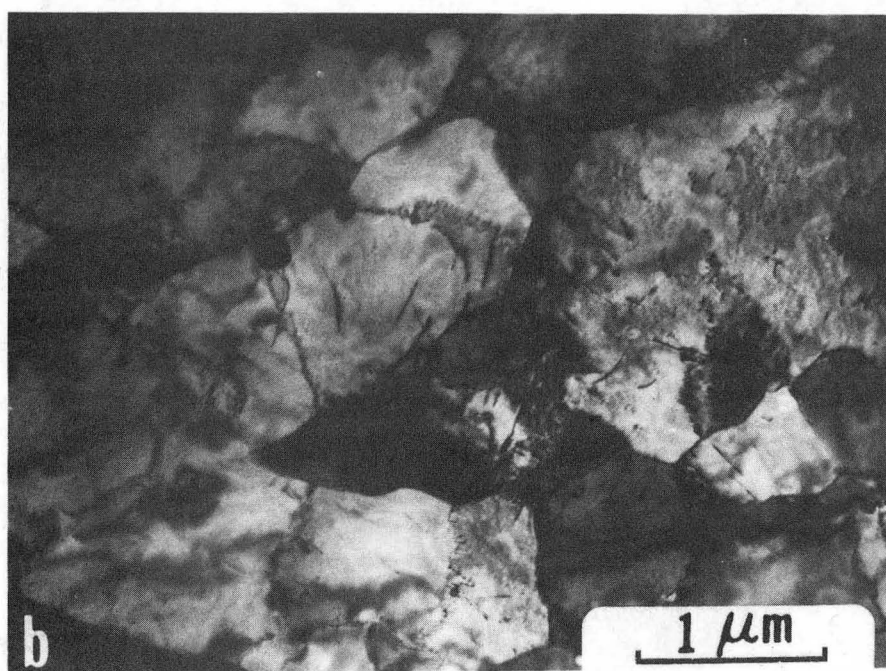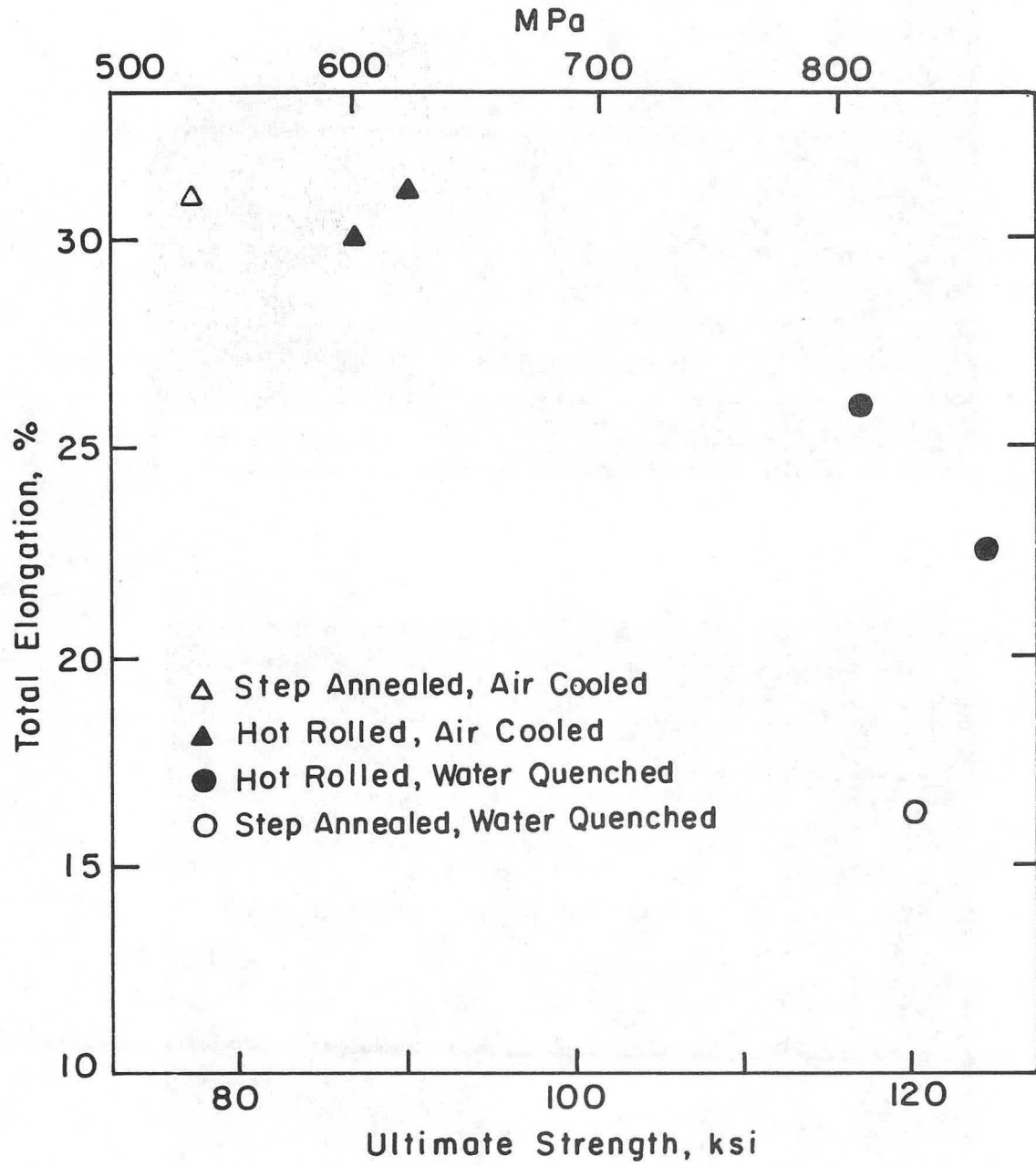
XBL 837-6016

Fig. 27
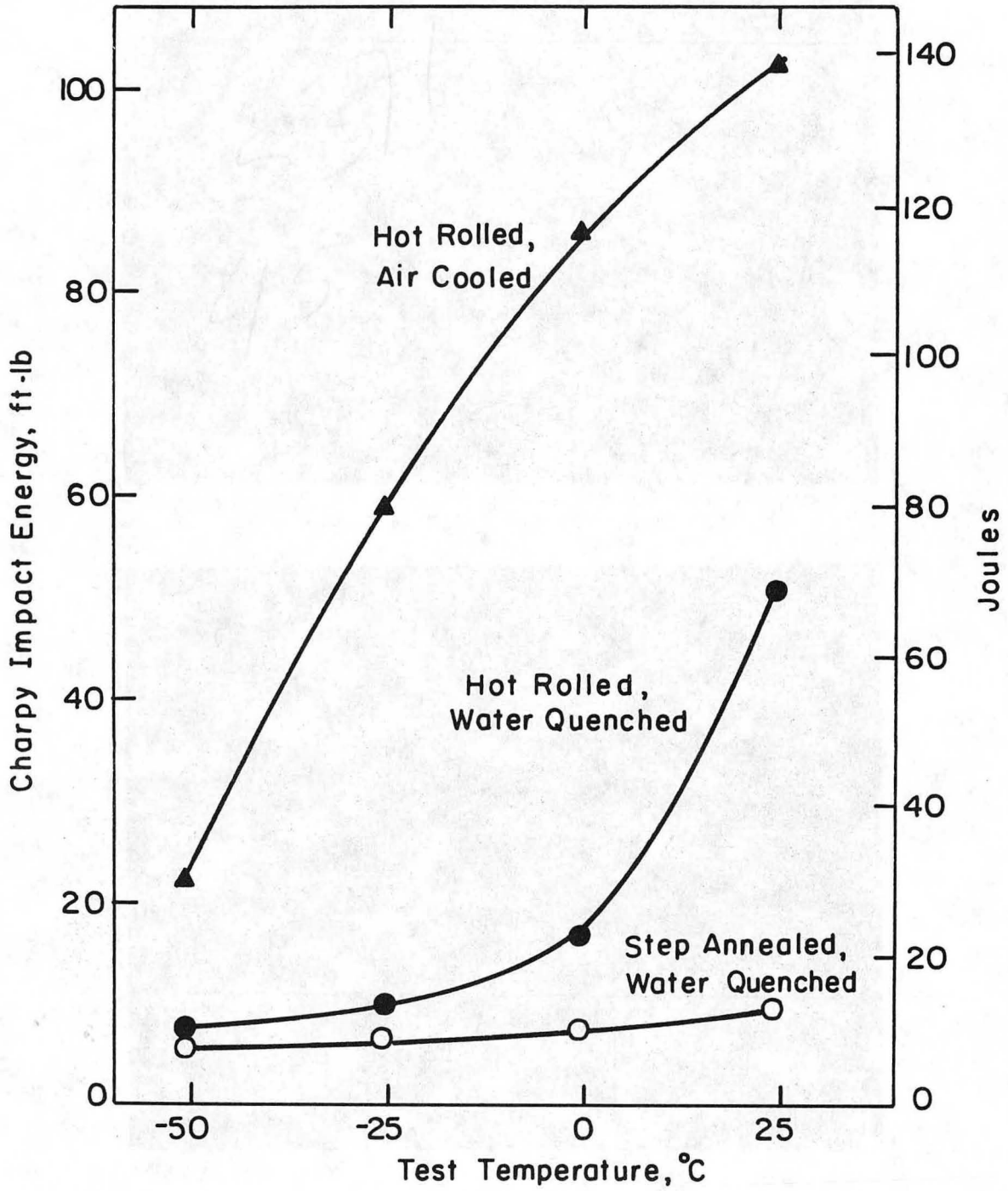
XBL 837-6015

Fig. 28
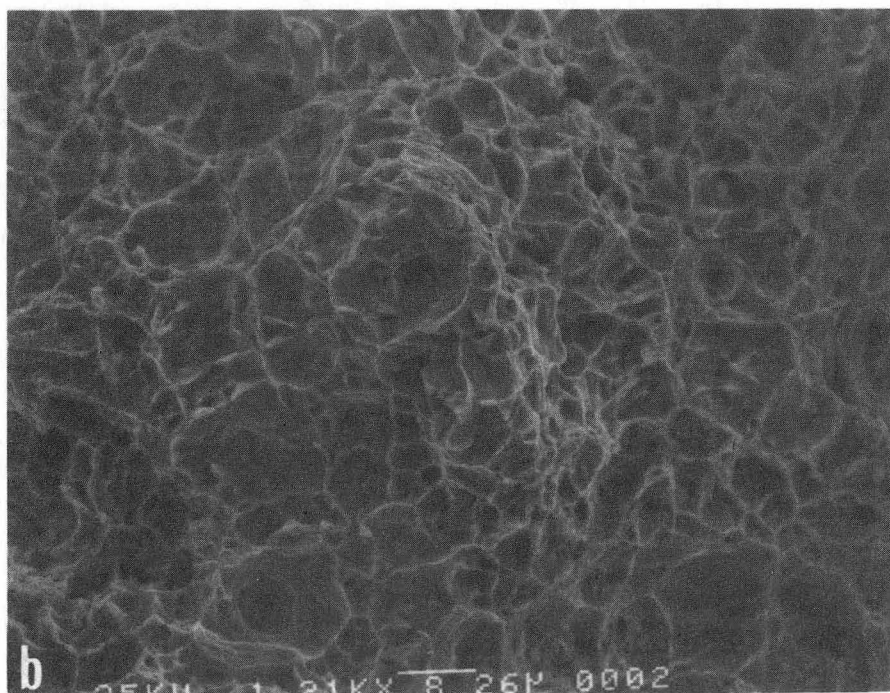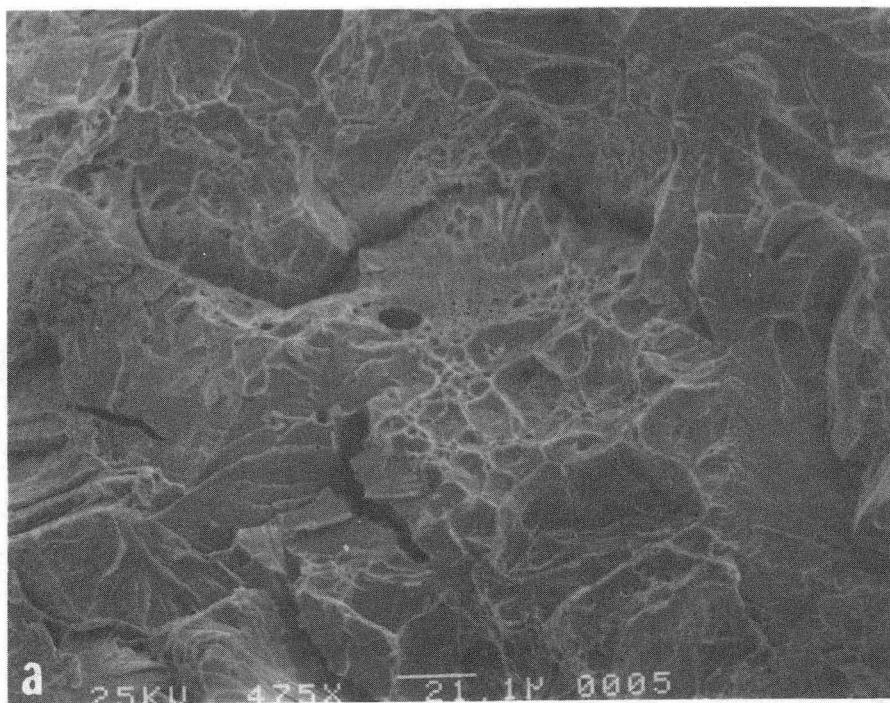
XBB 837-6260

Fig. 29
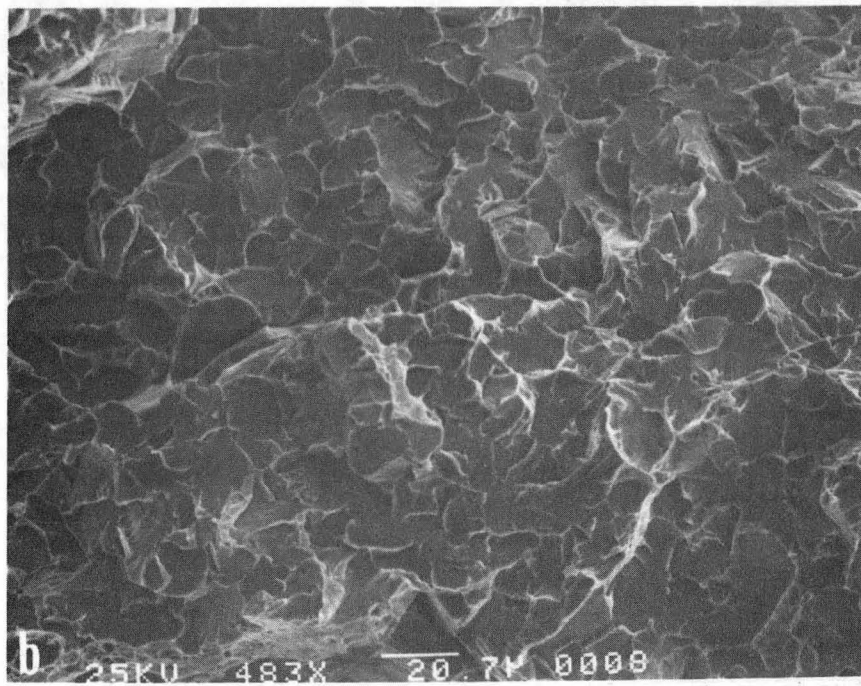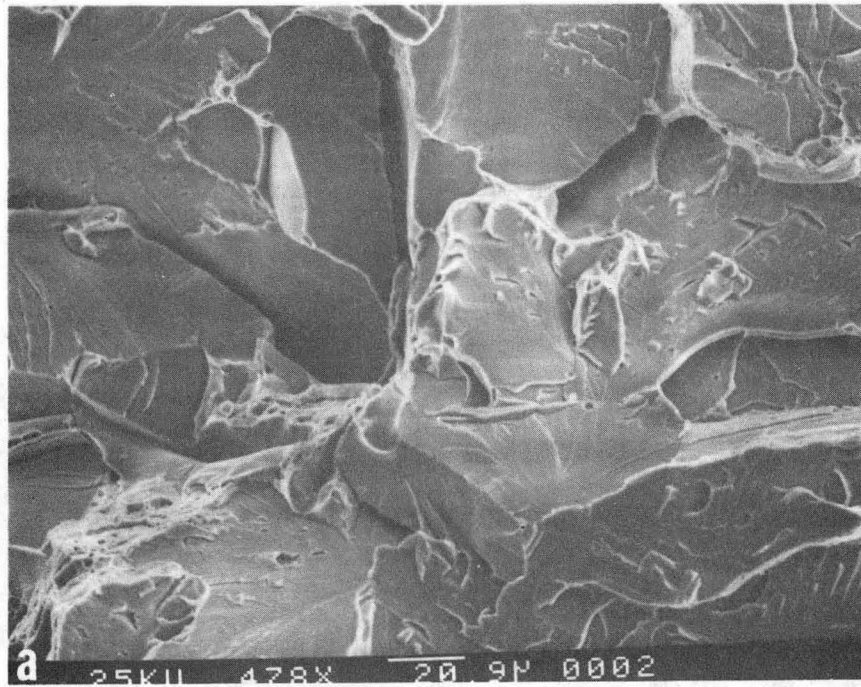
XBB 837-6261

Fig. 30
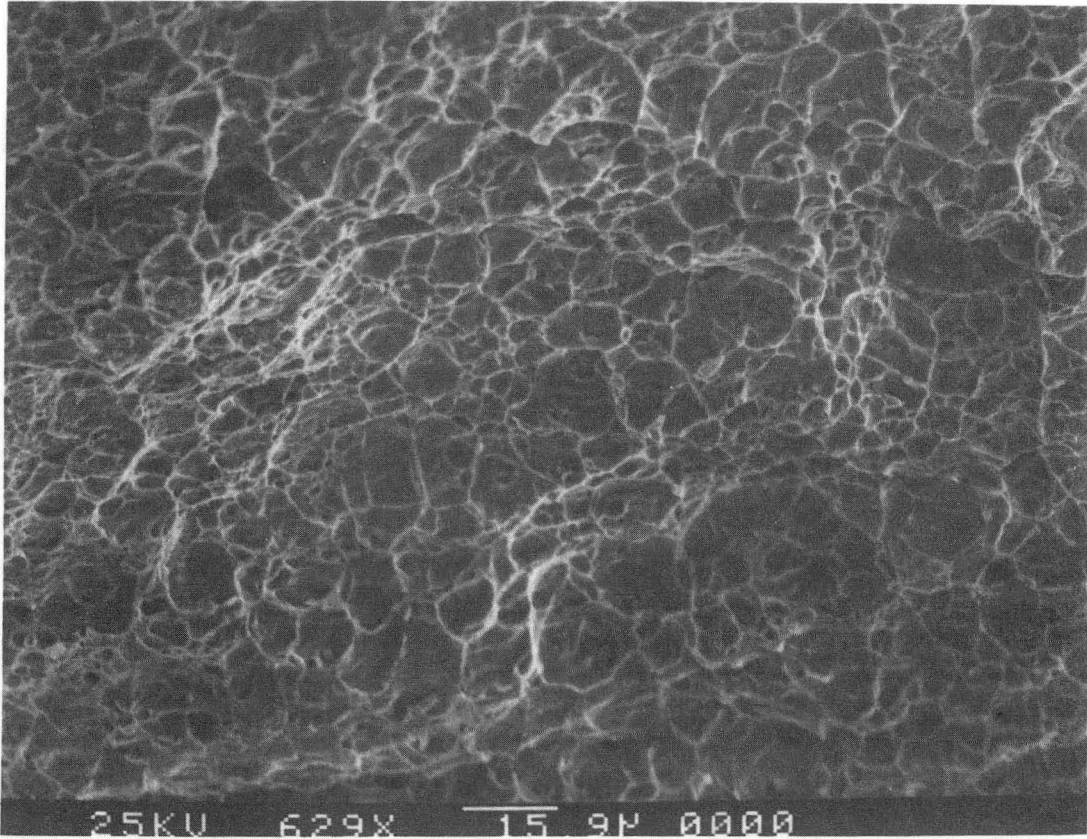
XBB 837-6269

Fig. 31

XBB 837-6262

Fig. 32

25KU   244X   41.0M 0007

25KU   482X   20.7M 0010

XBB 837-6263

Fig. 33